Nayana OCR: A Scalable Framework for Document OCR in Low-Resource Languages

Adithya S Kolavi[1], Samarth P[1], Vyoman Jain[1]

[1]CognitiveLab

Correspondence: adithyaskolavi@gmail.com, samarthprakash8@gmail.com, vyomanjain@gmail.com

Abstract

We introduce Nayana, a scalable and efficient framework for adapting Vision-Language Models (VLMs) to low-resource languages. Despite significant advances, modern VLMs remain constrained by the scarcity of training data in non-English languages, limiting their global applicability. Our framework addresses this fundamental challenge through a novel layout-aware synthetic data generation pipeline combined with parameter-efficient adaptation techniques. Instead of requiring extensive manually annotated datasets, Nayana enables existing models to learn new languages effectively using purely synthetic data. Using Low-Rank Adaptation (LoRA), we demonstrate this capability across ten Indic languages: Bengali, Gujarati, Hindi, Kannada, Malayalam, Marathi, Odia, Punjabi, Tamil, and Telugu. Through extensive experiments in OCR tasks, we show that models can achieve strong performance in new languages without the traditional requirements of large-scale annotated datasets or extensive model modifications. Nayana's success in adapting VLMs to new languages with synthetic data establishes a practical pathway for extending AI capabilities to underserved language communities, particularly in scenarios where annotated data is scarce or unavailable.

1 Introduction

Vision-Language Models (Wang et al. (2024); Wu et al. (2024); Abdin et al. (2024); Chen et al. (2024); Liu et al. (2024a); Wei et al. (2024a)) have demonstrated remarkable success in high-resource languages like English. However, these advancements have not translated across all languages due to a fundamental challenge: the scarcity of high-quality training data. This limitation is particularly evident in languages with complex scripts, where creating large-scale manually annotated datasets is both time-consuming and prohibitively expensive. This has limited the adoption of VLMs for document understanding tasks across diverse languages.

Nayana is an adaptive framework designed to bridge this gap by enabling existing VLMs to learn new languages effectively without requiring extensive annotated datasets. While this paper demonstrates Nayana's capabilities through OCR tasks across ten Indic languages, the framework's approach is inherently flexible and can extend to other tasks and language families. Our methodology eliminates the traditional requirement of annotation by combining synthetic data generation with efficient model adaptation techniques.

The main contributions of this paper are:

1. **Novel Synthetic Data Generation Pipelines:** A layout-aware synthetic data generation pipeline that automates the creation of training datasets while preserving visual and structural relationships in documents. This approach significantly reduces the dependency on manually annotated data for low-resource languages.

2. **Systematic Analysis of LoRA-based Adaptation:** We conduct a comprehensive evaluation of different LoRA techniques and configurations to determine their effectiveness in multilingual adaptation. Our analysis explores whether supervised fine-tuning can enhance language transfer and identifies the optimal configurations for adapting VLMs to new languages with minimal computational overhead.

3. **Comprehensive Empirical Validation:** Through extensive experimentation and evaluation across ten Indic languages, we provide strong evidence that our synthetic data approach matches the performance of traditional OCR Models, establishing a scalable path forward for language adaptation in VLMs.

2 Related Work

Recent Vision Language Models like Qwen 2.5 VL (Wang et al., 2024), Deepseek-VL2 (Wu et al., 2024), InternVL 2.5 (Chen et al., 2024), Llava-NeXT (Liu et al., 2024a), Phi 3.5 Vision (Abdin et al., 2024) have advanced significantly in OCR, captioning, and visual question answering (Antol et al., 2015). These developments stem from parameter-efficient fine-tuning, synthetic data generation, and improved multimodal architectures.

Parameter-efficient fine-tuning methods are crucial for adapting VLMs to specific tasks and languages. Low-Rank Adaptation (Hu et al., 2021) enables efficient parameter updates through low-rank matrix injection in transformer layers.

Multilingual OCR and document understanding have progressed substantially, with systems like Tesseract (Smith, 2007) and PaddleOCR (Du et al., 2020) establishing foundations for multilingual text recognition. Transformer-based approaches like ViLanOCR (Cheema et al., 2024) leverage synthetic data for improved performance on underrepresented languages, while LLaVA-NeXT (Liu et al., 2024a) advances OCR through high-resolution processing and improved visual instruction tuning for training.

Synthetic data generation addresses data scarcity in low-resource settings. SynthVLM (Liu et al., 2024b) uses diffusion models to create image-text pairs, while DocSynth300K (Zhao et al., 2024) demonstrates the effectiveness of generated data for document understanding tasks.

OCR-free approaches offer alternatives to traditional pipelines. DocPedia (Feng et al., 2024) processes documents in the frequency domain, while TextHawk2 (Yu et al., 2024) employs decoder-only architecture with efficient tokenization. Solutions like DocLayout-YOLO (Zhao et al., 2024), Donut (Kim et al., 2021) and Nougat (Blecher et al., 2023) have also explored document understanding without traditional OCR models.

Despite advances in parameter-efficient fine-tuning, synthetic data generation, and OCR-free approaches, challenges persist in adapting VLMs to low-resource languages. Our work introduces language-agnostic synthetic pipelines, combines parameter-efficient tuning with high-resolution vision encoders, and extends OCR-free paradigms to low-resource languages.

3 Synthetic Data Generation: A Scalable Cross-Lingual Framework

The cornerstone of our work lies in developing a sophisticated pipeline for generating high-fidelity synthetic training data that preserves the intricate relationships between document layout, visual elements, and textual content across languages. Our framework addresses the fundamental challenge of data scarcity in low-resource languages through a novel approach that combines advanced document understanding, a state-of-the-art English OCR model, and context-aware translation mechanisms. This section details the architectural components and methodological innovations that enable scalable, high-quality dataset generation for multilingual document understanding tasks.

The pipeline's design emphasizes three critical aspects: preservation of document structure and visual hierarchy, accurate text recognition across diverse scripts, and contextually appropriate translation that maintains semantic integrity. Through careful orchestration of these elements, we achieve a system capable of generating training data that closely mirrors the complexity and nuance of naturally occurring documents while scaling efficiently across multiple languages and document types.

3.1 Seed Dataset Collection

The foundation of our synthetic data generation pipeline rests upon a meticulously curated corpus of English-language documents, encompassing approximately 14,000 distinct samples. Our primary source materials comprise research papers from arXiv (2,000 documents), medical literature from PubMed (1,000 documents), newspaper articles (1,000 pages), and marketing materials (10,000 samples). This collection represents a strategic balance across multiple domains and document types, carefully selected to capture the diverse spectrum of real-world document layouts, content structures and ensures comprehensive coverage of various typographical elements, structural patterns, and domain-specific formatting conventions that characterize modern document ecosystems.

The academic papers, drawn from arXiv's extensive repository, provide exemplars of complex multi-column layouts, mathematical notation, and intricate figure-text relationships. Medical literature from PubMed introduces specialized terminology and standardized reporting formats, while newspaper pages contribute examples of dynamic

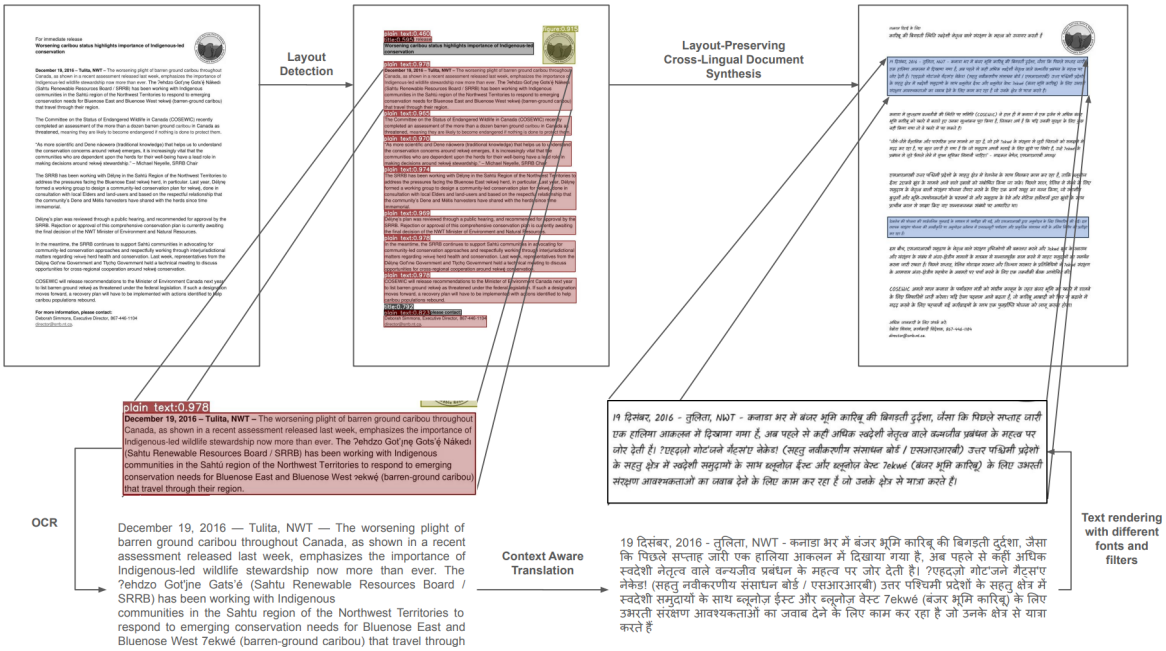

Figure 1: Nayana's end-to-end synthetic data generation pipeline. Starting from English document images, our pipeline generates multilingual datasets for OCR and Document level OCR tasks while preserving layout integrity and visual characteristics. The pipeline processes approximately one image every 3-5 seconds, enabling rapid dataset generation at scale.

layout patterns and diverse content organization. Marketing materials round out the collection with their rich variety of creative layouts, typographical treatments, and visual design elements.

3.2 Multi-stage Processing Pipeline

Our processing methodology employs a sophisticated multi-stage approach that preserves document integrity while enabling efficient multilingual adaptation. The pipeline initiates with high-resolution document preprocessing, converting all inputs to standardized 300 DPI images to ensure consistent quality and feature preservation across source formats. This standardization step establishes a robust foundation for subsequent processing stages.

The layout analysis phase employs an optimized implementation of DocLayout-YOLO (Zhao et al. (2024)), which systematically identifies and classifies document regions including text blocks, titles, figure captions, tables, and visual elements. While our initial research explored ensemble-based approaches using multiple layout detection models, empirical evaluation demonstrated that our optimized single-model implementation achieves comparable accuracy with significantly reduced computational overhead.

Text extraction and visual analysis proceed through a carefully orchestrated sequence of operations. Each identified text region undergoes precise optical character recognition to extract English text from our diverse document collection. We selected Tesseract (Smith (2007)) as the pipeline's OCR model amongst state-of-the-art candidates including PaddleOCR (Du et al. (2020)) and EasyOCR due to its high accuracy at low compute expenditure. The extracted text then undergoes comprehensive visual attribute analysis. This includes background and text color detection, font size estimation, and preservation of critical styling metadata. Our implementation maintains strict fidelity to the original document's visual hierarchy and structural relationships throughout this process.

The translation phase employs a sophisticated multi-engine approach, leveraging several state-of-the-art translation services: Google Translate API, Microsoft Azure Translate, IndicTrans2 (Gala et al. (2023)), and advanced language models such as Llama3.1 405B (Dubey et al. (2024)). This diverse ensemble of translation engines enables robust context-aware translation, with each service contributing its unique strengths in handling different aspects of document context, technical terminology, and formatting conventions.

Our system dynamically selects the most appropriate translation based on context, domain, and

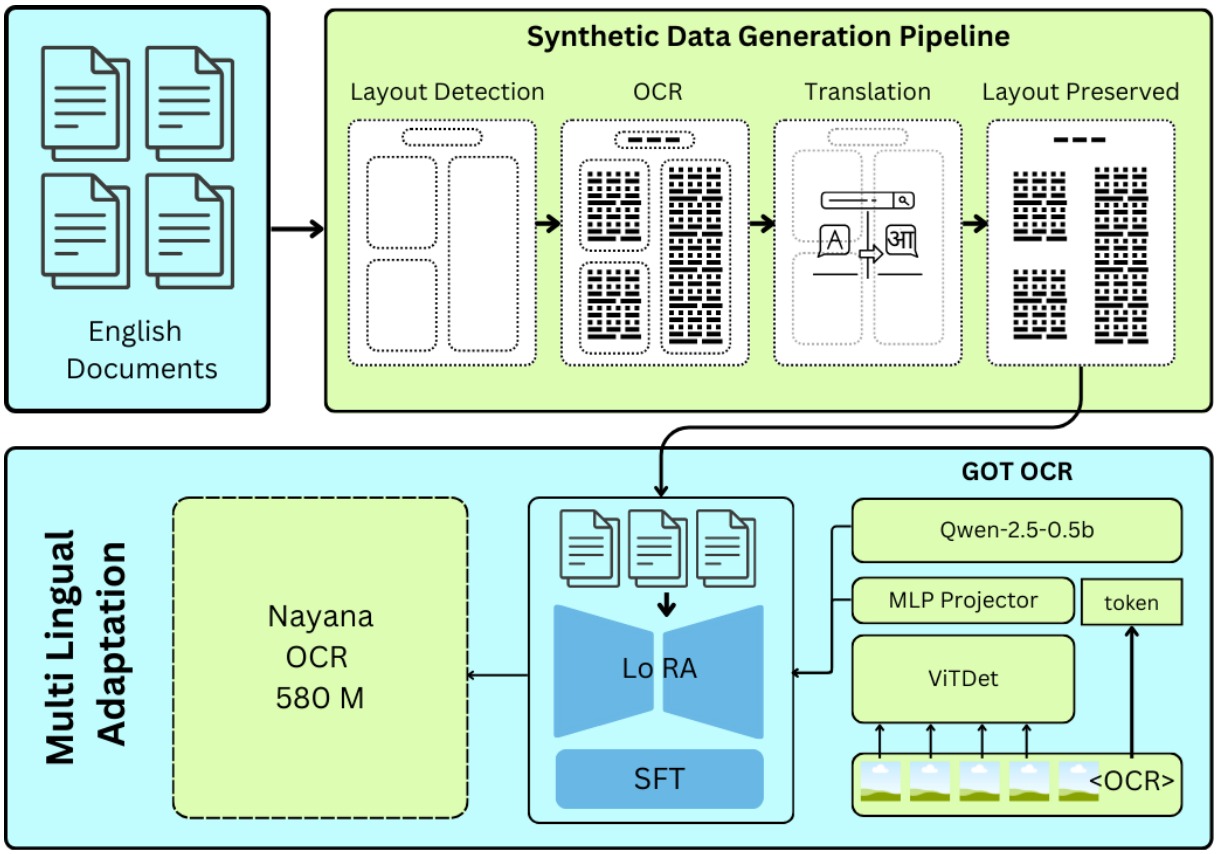

Figure 2: End-to-end Nayana system architecture: (1) A synthetic data generation pipeline transforming English documents into multilingual training data while preserving layout and visual fidelity, (2) OCR model with LoRA adapters for efficient multilingual adaptation, and (3) Training pipeline with Supervised Fine-Tuning (SFT). The modular architecture processes documents in 3-5 seconds while enabling rapid adaptation to new languages with high accuracy.

language pair, ensuring optimal translation quality across diverse document types. The final stage involves precise layout-preserving text replacement (Zhao et al. (2024)), incorporating dynamic font size adjustments and maintaining visual hierarchy while ensuring color contrast preservation.

3.3 Pipeline Performance Characteristics

Our pipeline achieves remarkable efficiency metrics, demonstrating both speed and accuracy at scale. Processing individual documents in approximately 3-5 seconds, the system maintains exceptional performance across all processing stages while enabling rapid dataset generation for new languages. The optimized DocLayout-YOLO (Zhao et al. (2024)) implementation consistently achieves 95.8% accuracy in structural analysis, while the OCR model and sophisticated translation architecture work in concert to ensure high-quality text extraction and translation.

The system's effectiveness is particularly evident in its data multiplication capabilities. Through our augmentation strategies and multi-task generation approach where we use the layout data to extract region-specific information, we achieve an output multiplication factor of 7-10× images per source document. This rich extraction process yields diverse training signals including layout structures, text content. The extracted multi-modal elements can be leveraged for training various downstream models such as VLMs for Visual Question Answering (Antol et al., 2015), Information Extraction systems, Multi-Modal Retrievers(Faysse et al., 2025).This multiplication effect significantly amplifies the utility of our seed dataset, enabling the creation of comprehensive training sets from a relatively modest collection of source documents. The combination of speed, multiplication factor, and rich multi-modal data extraction makes our pipeline particularly effective for rapidly bootstrapping vision-language capabilities in new languages and diverse document understanding applications.

4 Architectural Innovation: Parameter-Efficient Cross-Script Learning

The adaptation of vision-language models (VLMs) for multilingual document understanding presents a fundamental architectural challenge: How to effectively extend models trained primarily on Latin scripts to handle dramatically different writing systems while maintaining computational efficiency. This section details our systematic exploration of architectural approaches, empirically-driven design decisions, and the development of our parameter-efficient adaptation methodology.

Our initial investigation began with a comprehensive evaluation of contemporary VLM architectures, analyzing their fundamental capabilities in handling text-dense images. This exploration revealed a critical insight: while many models excel at general visual understanding, they often struggle with the precise geometric and spatial relationships inherent in document processing. Through extensive experimentation with architectures ranging from traditional CNN-based models to state-of-the-art transformer variants, we identified several key architectural requirements that would prove crucial for successful cross-script adaptation.

4.1 Foundation Model Selection and Analysis

The selection of an appropriate foundation model emerged from a rigorous empirical study evaluating multiple state-of-the-art architectures. Our investigation focused particularly on models' ability to handle the unique challenges presented by Indic scripts, including complex ligatures, overlapping characters, and varied writing directions. Initial experiments with popular vision-language models revealed significant limitations in handling dense textual content, despite their strong performance on general vision-language tasks.

The breakthrough came through our analysis of GOT OCR (580M parameters) (Wei et al. (2024b)), which demonstrated exceptional performance across key metrics. Based on published benchmarks, GOT OCR achieved superior results with an Edit Distance of 0.035/0.038 and F1-scores of 0.972/0.980 for English and Chinese respectively, significantly outperforming larger models like Qwen-VL-Max (>72B parameters) (Wang et al. (2024)) and Vary (7B parameters) (Wei et al. (2024a)). More importantly, its architecture demonstrated remarkable flexibility in handling non-Latin scripts, likely due to its original design for handling both English and Chinese characters – writing systems with significantly different visual characteristics.

Our choice of GOT OCR (Wei et al. (2024b)) was further validated through its optimal balance of performance and efficiency due to its:

- Superior vision transformer backbone architecture compared to contemporary VLM designs
- Specialized text detection heads optimized for dense textual content
- Efficient parameter count (580M) enabling practical deployment while maintaining state-of-the-art performance

The model's architecture, particularly its attention mechanisms and hierarchical feature processing, provided an ideal foundation for our cross-script adaptation strategy. Notably, its transformer-based design facilitated efficient parameter adaptation through Low-Rank Adaptation (Hu et al. (2021)), enabling us to preserve the model's fundamental visual understanding while extending its capabilities to new scripts.

During our initial exploration phase, we pursued several alternative approaches that, while ultimately unsuccessful, provided crucial insights. We conducted extensive experiments with vocabulary expansion techniques, hypothesizing that direct modification of the tokenization layer would enable better handling of Indic scripts. These experiments involved:

- Direct vocabulary expansion with script-specific tokens
- Hierarchical tokenization schemes for handling complex ligatures
- Script-aware embedding layer modifications

Despite systematic exploration of these approaches with various hyperparameter configurations, the results consistently plateaued at 50-60% accuracy for both training and evaluation. This empirical evidence led us to a crucial realization: the challenge lay not in the vocabulary representation but in the fundamental visual processing of different scripts.

4.2 Cross-Modal Alignment Learning

The Cross-Modal Alignment (CMA) phase extends GOT OCR's (Wei et al., 2024b) capabilities beyond its original English and Chinese training domain through a two-phase training approach. Built on GOT OCR's task-token architecture (e.g., <OCR>), our adaptation strategy systematically builds multilingual capabilities while preserving the model's core strengths.

The first phase focuses on section-level training 15, where we use layout-preserving translation to create training pairs from dense textual sections. By unfreezing all major components (ViTDet vision encoder, MLP projection layer, and Qwen 0.5B language model), we enable comprehensive adaptation to new language patterns. Ablation studies confirmed this phase's criticality - attempts to skip directly to document-level training resulted in stalled learning and hallucinations.

The second phase transitions to document-level OCR 10, training on complete document images while selectively freezing components. We maintain the trained visual features by freezing the ViTDet vision encoder while continuing to train the language model and projection layer. This approach successfully extends the model's capabilities to new languages while preserving its performance on English and Chinese texts.

Table 1: Training Phase Configuration Summary

Component	Phase 1	Phase 2
ViTDet Vision Encoder	Unfrozen	Frozen
MLP Projection Layer	Unfrozen	Unfrozen
Qwen 0.5B LLM	Unfrozen	Unfrozen
Training Data	Text-heavy Sections	Complete Documents

4.3 Single-Language Adaptation Results

4.3.1 Hindi Adaptation Performance

Our initial experiments with Hindi adaptation revealed several crucial insights about parameter-efficient adaptation strategies. The choice of 85,000 image-text pairs was determined through extensive preliminary testing, which showed that this dataset size provided optimal coverage of Hindi script variations while remaining computationally manageable.

The results in Table 2 demonstrate a clear progression in adaptation effectiveness across different configurations. The baseline LoRA configuration (r=32, α =64) established fundamental script adaptation but showed limitations in handling complex Hindi character combinations, as evidenced by its BLEU score of 0.29. The optimal configuration (r=64, α=128) achieved substantially better performance, with a BLEU score of 0.58, through improved capacity for modeling intricate script-specific features.

Particularly noteworthy is the preservation of English language capabilities. While the higher-rank LoRA configuration showed a slight decrease in English BLEU scores (from 0.84 to 0.79), it maintained strong overall performance (F1: 0.86, METEOR: 0.88), suggesting effective balance between adaptation and preservation of base capabilities.

Table 2: Hindi Adaptation Performance Comparison

Configuration	Lang	BLEU↑	ANLS↑	F1↑	METEOR↑
LoRA	Hindi	0.29	0.71	0.56	0.57
(r=32, α=64)	English	0.84	0.97	0.91	0.91
LoRA	Hindi	**0.58**	**0.91**	**0.76**	**0.77**
(r=64, α=128)	English	0.79	0.97	0.86	0.88
Full	Hindi	0.50	0.86	0.75	0.73
Fine-tune	English	0.74	0.95	0.85	0.85

4.3.2 Tamil Adaptation Performance

The Tamil adaptation experiments presented unique challenges due to the script's distinctive characteristics, including its cursive nature and complex grapheme structure. Table 3 reveals several important patterns in adaptation behavior. The LoRA configuration (r=64, α=128) demonstrated remarkable robustness in handling Tamil's unique script features, achieving a BLEU score of 0.37 despite the script's significant divergence from the model's original training domain. This performance is particularly impressive given Tamil's complex vowel modification system and the presence of compound characters that can span multiple positions. The comparison with full fine-tuning is especially illuminating. While full fine-tuning achieved reasonable performance (ANLS: 0.79), it showed significant degradation in English capabilities, suggesting potential catastrophic forgetting. In contrast, our LoRA approach maintained strong performance across both languages, with English metrics remaining notably stable (BLEU: 0.78, F1: 0.87).

4.4 Multi-Language Adaptation

We investigated three distinct approaches to handling multiple scripts simultaneously, each offering unique insights into cross-lingual transfer. The Single LoRA approach emerged as particularly effective, demonstrating strong performance across

Table 3: Tamil Adaptation Performance Comparison

Configuration	Lang	BLEU↑	ANLS↑	F1↑	METEOR↑
LoRA	Tamil	**0.37**	**0.87**	**0.66**	**0.64**
(r=64, α=128)	English	**0.78**	**0.96**	**0.87**	**0.88**
Full	Tamil	0.17	0.79	0.44	0.44
Fine-tune	English	0.69	0.96	0.76	0.80

multiple languages without requiring explicit language specification during inference. When language tags were provided both during training and inference, we observed further improvements in performance. A notable advantage of this approach was its ability to leverage cross-script learning - for instance, the model showed improved handling of Marathi text despite being primarily trained on Hindi, suggesting effective transfer between related Devanagari scripts. The Multi-LoRA approach, training separate LoRA modules for each language, achieved strong language-specific performance but sacrificed the beneficial cross-script transfer effects observed in the single LoRA strategy. Despite its strong per-language performance, this approach's inability to leverage script similarities represented a significant limitation in the multilingual context. Nayana We also explored a Merged LoRA strategy, where independently trained language-specific LoRAs were combined using model merging techniques. While this approach showed promising results for both languages, it did not outperform the single LoRA approach's ability to capture cross-script features.

Table 4: Multi-Language Adaptation Performance (Hindi + Kannada) in a single LoRA

Configuration	Lang	BLEU↑	ANLS↑	F1↑	METEOR↑
Single	Hindi	0.64	0.89	0.85	0.84
LoRA	Kannada	0.52	0.72	0.55	0.43
	English	0.79	0.97	0.86	0.88

5 Results

5.1 Evaluation Methodology

Our evaluation framework was designed to provide rigorous, comprehensive assessment across diverse document types and writing systems. We constructed a carefully balanced test set comprising 500 images per language, strategically distributed across different document categories to ensure broad coverage of real-world scenarios. The dataset draws 40% of its content from academic papers sourced from arXiv, another 40% from medical literature in PubMed, and the remaining 20% split equally between newspaper content and advertising materials. This distribution reflects the varying complexity and specialized requirements of different document processing applications.

To ensure methodological rigor and fair cross-linguistic comparison, we developed parallel versions of each document across all ten languages while maintaining identical visual layouts and content structures. This parallel corpus approach enables precise isolation of script-specific challenges while controlling for variations in document complexity and formatting. Such controlled comparison proves essential for understanding the true impact of script differences on model performance.

5.2 Comparative Analysis

Our comprehensive evaluation framework encompasses three distinct categories of document processing systems, each representing different approaches to multilingual document understanding. We first examined traditional OCR systems, including industry standards like Tesseract Smith (2007) and PaddleOCR (Du et al. (2020)), which have established strong baselines in multilingual text recognition. These systems, while specialized for OCR tasks, provide important reference points for performance evaluation.

The second category comprises recent vision-language models, including cutting-edge systems like Phi-3.5 Vision (Abdin et al. (2024)) and Llama-3.2 (Dubey et al. (2024)). These models, despite their impressive capabilities in general vision-language tasks, demonstrate the ongoing challenges in specialized document processing. Our analysis of their performance reveals important insights about the limitations of general-purpose architectures when applied to script-specific document understanding tasks.

Our Nayana-OCR variants, built upon the GOT OCR (Wei et al. (2024b)) architecture, represent the third category. Through extensive training on approximately 850,000 synthetic images spanning 10 Indic languages, these models demonstrate significant advantages in multilingual document processing. The results reveal substantial improvements across key metrics, most notably a 76% reduction in Character Error Rate compared to the base GOT OCR model. This improvement is particularly significant given that it maintains consistency across all evaluated languages.

The performance gains extend beyond simple

Table 5: Average performance metrics across all evaluated languages. Results show mean values for each model across the ten tested languages. Lower values (↓) are better for CER and WER, while higher values (↑) are better for other metrics. Best results in each category are highlighted in **bold**.

Model	CER↓	WER↓	BLEU↑	ANLS↑	METEOR↑
Tesseract	**0.206**	0.583	0.318	**0.797**	0.540
PaddleOCR	0.621	0.880	0.020	0.287	0.069
Llama-3.2 11B	3.858	3.900	0.007	0.091	0.055
Phi-3.5 Vision	2.420	2.461	0.007	0.086	0.044
Qwen2-VL 2B	1.776	1.793	0.025	0.129	0.086
GOT-OCR	0.945	1.041	0.016	0.071	0.052
Nayana-OCR	0.227	**0.463**	**0.395**	**0.796**	**0.630**

character recognition. Our models show markedly improved BLEU scores, indicating enhanced capability in handling complex linguistic structures and maintaining semantic coherence. The reduced standard deviations across performance metrics suggest robust cross-language stability, a crucial factor for practical deployment in multilingual environments. These improvements stem from our innovative approach to model adaptation and the sophisticated synthetic data generation pipeline described in previous sections.

5.3 Detailed Performance Analysis

Examining Table 6, several patterns emerge that illustrate the strengths and limitations of different approaches. Traditional OCR systems like Tesseract (Smith (2007)) show strong performance in character-level accuracy (CER: 0.206) but struggle with higher-level semantic understanding, as evidenced by lower BLEU scores (0.318). In contrast, Nayana-OCR achieves competitive character-level accuracy (CER: 0.227) while substantially outperforming all baselines in semantic metrics (BLEU: 0.395).

The performance gap between general-purpose vision-language models and specialized OCR systems is particularly noteworthy. Despite their larger parameter counts, models like Llama-3.2 11B (Dubey et al. (2024)) and Phi-3.5 Vision (Abdin et al. (2024)) show significantly higher error rates across all metrics. This disparity underscores the importance of architectural choices specifically optimized for document understanding tasks.

5.4 Limitations and Future Work

While our approach demonstrates significant progress, several limitations should be noted. When compared to traditional OCR systems, our models show higher inference latency, reflecting the complexity of vision-language processing. Performance variations across scripts suggest room for improvement in handling certain complex writing systems. Additionally, our synthetic data generation, while efficient, may not capture all real-world variations in document layouts and styles.

Future work will focus on expanding the diversity of seed datasets, incorporating more complex document structures, and developing specialized architectures that better balance performance and computational efficiency. We also plan to explore how our synthetic data approach can benefit other vision-language tasks and create open-source tools to facilitate broader adoption of multilingual vision-language technologies.

6 Conclusion

This work establishes that vision-language models can be effectively adapted to new languages using purely synthetic data, reducing dependency on costly manual annotation. Our results demonstrate that Nayana provides a practical, scalable solution for extending AI capabilities to low-resource languages. By achieving strong performance across diverse scripts while maintaining computational efficiency, our framework opens new possibilities for democratizing AI technologies across linguistic boundaries. The success of our approach not only validates the effectiveness of synthetic data generation and efficient adaptation techniques but also establishes a promising direction for developing more inclusive AI systems that can serve diverse linguistic communities worldwide.

References

Marah Abdin, Jyoti Aneja, Hany Awadalla, Ahmed Awadallah, Ammar Ahmad Awan, Nguyen Bach, Amit Bahree, Arash Bakhtiari, Jianmin Bao, Harkirat Behl, et al. 2024. Phi-3 technical report: A highly capable language model locally on your phone. *arXiv preprint arXiv:2404.14219*.

Stanislaw Antol, Aishwarya Agrawal, Jiasen Lu, Margaret Mitchell, Dhruv Batra, C Lawrence Zitnick, and Devi Parikh. 2015. Vqa: Visual question answering. In *Proceedings of the IEEE international conference on computer vision*, pages 2425–2433.

Lukas Blecher, Guillem Cucurull, Thomas Scialom, and Robert Stojnic. 2023. Nougat: Neural optical understanding for academic documents. *arXiv preprint arXiv:2308.13418*.

Musa Dildar Ahmed Cheema, Mohammad Daniyal Shaiq, Farhaan Mirza, Ali Kamal, and M Asif Naeem. 2024. Adapting multilingual vision language transformers for low-resource urdu optical character recognition (ocr). *PeerJ Computer Science*, 10:e1964.

Zhe Chen, Jiannan Wu, Wenhai Wang, Weijie Su, Guo Chen, Sen Xing, Muyan Zhong, Qinglong Zhang, Xizhou Zhu, Lewei Lu, et al. 2024. Internvl: Scaling up vision foundation models and aligning for generic visual-linguistic tasks. In *Proceedings of the IEEE/CVF Conference on Computer Vision and Pattern Recognition*, pages 24185–24198.

Yuning Du, Chenxia Li, Ruoyu Guo, Xiaoting Yin, Weiwei Liu, Jun Zhou, Yifan Bai, Zilin Yu, Yehua Yang, Qingqing Dang, et al. 2020. Pp-ocr: A practical ultra lightweight ocr system. *arXiv preprint arXiv:2009.09941*.

Abhimanyu Dubey, Abhinav Jauhri, Abhinav Pandey, Abhishek Kadian, Ahmad Al-Dahle, Aiesha Letman, Akhil Mathur, Alan Schelten, Amy Yang, Angela Fan, et al. 2024. The llama 3 herd of models. *arXiv preprint arXiv:2407.21783*.

Manuel Faysse, Hugues Sibille, Tony Wu, Bilel Omrani, Gautier Viaud, Céline Hudelot, and Pierre Colombo. 2025. Colpali: Efficient document retrieval with vision language models. *Preprint*, arXiv:2407.01449.

Hao Feng, Qi Liu, Hao Liu, Jingqun Tang, Wengang Zhou, Houqiang Li, and Can Huang. 2024. Docpedia: Unleashing the power of large multimodal model in the frequency domain for versatile document understanding. *Science China Information Sciences*, 67(12):1–14.

Jay Gala, Pranjal A Chitale, Raghavan AK, Varun Gumma, Sumanth Doddapaneni, Aswanth Kumar, Janki Nawale, Anupama Sujatha, Ratish Puduppully, Vivek Raghavan, et al. 2023. Indictrans2: Towards high-quality and accessible machine translation models for all 22 scheduled indian languages. *arXiv preprint arXiv:2305.16307*.

Edward J Hu, Yelong Shen, Phillip Wallis, Zeyuan Allen-Zhu, Yuanzhi Li, Shean Wang, Lu Wang, and Weizhu Chen. 2021. Lora: Low-rank adaptation of large language models. *arXiv preprint arXiv:2106.09685*.

Geewook Kim, Teakgyu Hong, Moonbin Yim, Jinyoung Park, Jinyeong Yim, Wonseok Hwang, Sangdoo Yun, Dongyoon Han, and Seunghyun Park. 2021. Donut: Document understanding transformer without ocr. *arXiv preprint arXiv:2111.15664*, 7(15):2.

Haotian Liu, Chunyuan Li, Qingyang Wu, and Yong Jae Lee. 2024a. Visual instruction tuning. *Advances in neural information processing systems*, 36.

Zheng Liu, Hao Liang, Xijie Huang, Wentao Xiong, Qinhan Yu, Linzhuang Sun, Chong Chen, Conghui He, Bin Cui, and Wentao Zhang. 2024b. Synthvlm: High-efficiency and high-quality synthetic data for vision language models. *arXiv preprint arXiv:2407.20756*.

Ray Smith. 2007. An overview of the tesseract ocr engine. In *ICDAR '07: Proceedings of the Ninth International Conference on Document Analysis and Recognition*, pages 629–633, Washington, DC, USA. IEEE Computer Society.

Peng Wang, Shuai Bai, Sinan Tan, Shijie Wang, Zhihao Fan, Jinze Bai, Keqin Chen, Xuejing Liu, Jialin Wang, Wenbin Ge, et al. 2024. Qwen2-vl: Enhancing vision-language model's perception of the world at any resolution. *arXiv preprint arXiv:2409.12191*.

Haoran Wei, Lingyu Kong, Jinyue Chen, Liang Zhao, Zheng Ge, Jinrong Yang, Jianjian Sun, Chunrui Han, and Xiangyu Zhang. 2024a. Vary: Scaling up the vision vocabulary for large vision-language model. In *European Conference on Computer Vision*, pages 408–424. Springer.

Haoran Wei, Chenglong Liu, Jinyue Chen, Jia Wang, Lingyu Kong, Yanming Xu, Zheng Ge, Liang Zhao, Jianjian Sun, Yuang Peng, et al. 2024b. General ocr theory: Towards ocr-2.0 via a unified end-to-end model. *arXiv preprint arXiv:2409.01704*.

Zhiyu Wu, Xiaokang Chen, Zizheng Pan, Xingchao Liu, Wen Liu, Damai Dai, Huazuo Gao, Yiyang Ma, Chengyue Wu, Bingxuan Wang, et al. 2024. Deepseek-vl2: Mixture-of-experts vision-language models for advanced multimodal understanding. *arXiv preprint arXiv:2412.10302*.

Ya-Qi Yu, Minghui Liao, Jiwen Zhang, and Jihao Wu. 2024. Texthawk2: A large vision-language model excels in bilingual ocr and grounding with 16x fewer tokens. *arXiv preprint arXiv:2410.05261*.

Zhiyuan Zhao, Hengrui Kang, Bin Wang, and Conghui He. 2024. Doclayout-yolo: Enhancing document layout analysis through diverse synthetic data and global-to-local adaptive perception. *arXiv preprint arXiv:2410.12628*.

A Appendix

A.1 Language-wise Performance Analysis

Table 6: Detailed Performance Analysis Across Languages. The table compares various OCR models across multiple languages using metrics such as CER, WER, BLEU, ANLS and METEOR.

Model	CER↓	WER↓	BLEU↑	ANLS↑	METEOR↑
Hindi					
Tesseract	**0.090**	**0.287**	**0.636**	**0.908**	**0.791**
PaddleOCR	0.414	0.864	0.023	0.575	0.117
Phi-3.5 Vision	2.878	2.500	0.023	0.126	0.069
Llama-3.2 11B	4.654	3.455	0.020	0.116	0.070
Qwen2-VL 2B	2.360	2.022	0.066	0.172	0.153
GOT OCR base	1.013	1.190	0.004	0.052	0.043
Nayana-OCR	0.160	0.297	0.532	0.850	0.756
Kannada					
Tesseract	**0.155**	**0.609**	0.259	**0.847**	0.541
PaddleOCR	0.814	0.918	0.020	0.110	0.048
Phi-3.5 Vision	2.655	2.877	0.006	0.084	0.046
Llama-3.2 11B	4.670	4.991	0.004	0.075	0.047
Qwen2-VL 2B	1.394	1.599	0.013	0.075	0.063
GOT OCR base	0.936	1.008	0.019	0.067	0.063
Nayana-OCR	0.361	0.648	**0.341**	0.740	**0.554**
Tamil					
Tesseract	0.265	0.811	0.109	0.750	0.324
PaddleOCR	0.545	1.076	0.003	0.450	0.051
Phi-3.5 Vision	1.531	2.033	0.000	0.082	0.035
Llama-3.2 11B	3.009	4.229	0.002	0.086	0.052
Qwen2-VL 2B	1.260	1.515	0.007	0.125	0.053
GOT OCR base	0.956	1.020	0.013	0.056	0.051
Nayana-OCR	**0.181**	**0.551**	**0.377**	**0.829**	**0.592**
Telugu					
Tesseract	**0.158**	0.589	**0.296**	**0.821**	**0.551**
PaddleOCR	0.435	0.934	0.014	0.550	0.088
Phi-3.5 Vision	2.442	2.464	0.001	0.067	0.036
Llama-3.2 11B	2.736	3.586	0.015	0.090	0.068
Qwen2-VL 2B	1.580	1.696	0.010	0.115	0.065
GOT OCR base	0.925	1.007	0.022	0.075	0.066
Nayana-OCR	0.282	**0.065**	0.241	0.733	0.522
Odia					
Tesseract	**0.290**	0.681	0.155	0.703	0.403
PaddleOCR	0.639	**0.742**	0.020	0.111	0.030
Phi-3.5 Vision	2.311	2.168	0.000	0.090	0.018
Llama-3.2 11B	2.880	2.908	0.005	0.088	0.042
Qwen2-VL 2B	1.247	1.345	0.012	0.092	0.060
GOT OCR base	0.926	1.000	0.020	0.078	0.042
Nayana-OCR	0.311	0.566	**0.305**	**0.738**	**0.551**

Model	CER↓	WER↓	BLEU↑	ANLS↑	METEOR↑
Punjabi					
Tesseract	0.203	0.532	0.356	0.803	0.568
PaddleOCR	0.717	0.811	0.010	0.095	0.029
Phi-3.5 Vision	3.431	2.896	0.001	0.083	0.034
Llama-3.2 11B	5.801	4.535	0.000	0.065	0.029
Qwen2-VL 2B	1.260	1.515	0.007	0.125	0.053
GOT OCR base	0.954	0.994	0.010	0.066	0.046
Nayana-OCR	**0.159**	**0.440**	**0.435**	**0.853**	**0.693**
Malayalam					
Tesseract	0.355	0.828	0.065	0.663	0.258
PaddleOCR	0.788	**0.895**	0.036	0.125	0.073
Phi-3.5 Vision	1.993	2.489	0.000	0.070	0.039
Llama-3.2 11B	2.988	3.807	0.001	0.081	0.051
Qwen2-VL 2B	1.394	1.599	0.013	0.075	0.063
GOT OCR base	0.956	1.174	0.011	0.064	0.047
Nayana-OCR	**0.270**	0.694	**0.248**	**0.740**	**0.516**
Marathi					
Tesseract	0.157	0.460	0.513	0.862	0.738
PaddleOCR	0.355	0.849	0.035	0.630	0.154
Phi-3.5 Vision	1.592	2.063	0.023	0.150	0.073
Llama-3.2 11B	2.421	2.724	0.007	0.108	0.074
Qwen2-VL 2B	1.251	1.269	0.069	0.248	0.181
GOT OCR base	0.915	0.988	0.021	0.095	0.060
Nayana-OCR	**0.143**	**0.457**	**0.540**	**0.866**	**0.753**
Gujarati					
Tesseract	**0.148**	0.446	**0.534**	**0.871**	**0.733**
PaddleOCR	0.800	0.914	0.026	0.124	0.068
Phi-3.5 Vision	3.329	3.008	0.006	0.091	0.047
Llama-3.2 11B	2.401	2.724	0.007	0.108	0.074
Qwen2-VL 2B	5.050	4.312	0.006	0.092	0.042
GOT OCR base	0.940	1.047	0.020	0.081	0.057
Nayana-OCR	0.172	**0.451**	0.476	0.839	0.707
Bengali					
Tesseract	0.241	0.590	0.259	0.738	0.492
PaddleOCR	0.704	0.798	0.014	0.096	0.029
Phi-3.5 Vision	2.041	2.110	0.008	0.014	0.042
Llama-3.2 11B	7.021	6.039	0.009	0.093	0.044
Qwen2-VL 2B	0.967	1.054	0.048	0.174	0.127
GOT OCR base	0.926	0.983	0.019	0.080	0.048
Nayana-OCR	**0.235**	**0.460**	**0.452**	**0.776**	**0.656**

A.2 Model Output Analysis

To evaluate the practical effectiveness of our model, we present a visual comparison between input documents and their corresponding Document Level OCR outputs. Figures 3 and 4 demonstrate the model's performance on Hindi and Bengali documents respectively.

The results demonstrate the model's robust performance across different Indic scripts. Note the preservation of both textual content and document structure in the generated outputs, highlighting the effectiveness of our approach in handling diverse document layouts and writing systems.

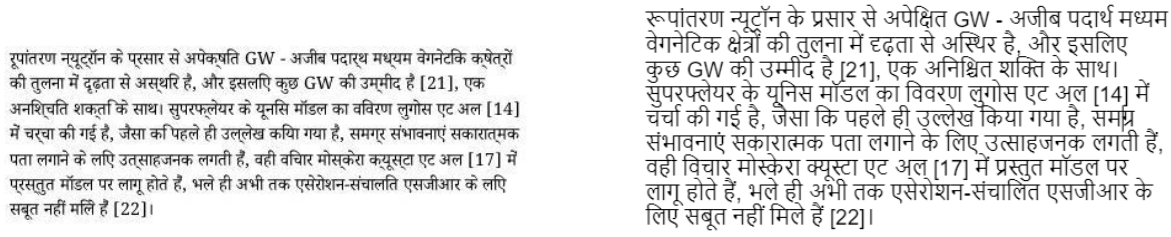

Figure 3: Hindi Document Processing: Comparison between the original document (left) and the model's OCR output (right), demonstrating accurate text recognition and formatting preservation.

Figure 4: Bengali Document Processing: Visual comparison showing the model's capability to accurately process Bengali script while maintaining structural fidelity.

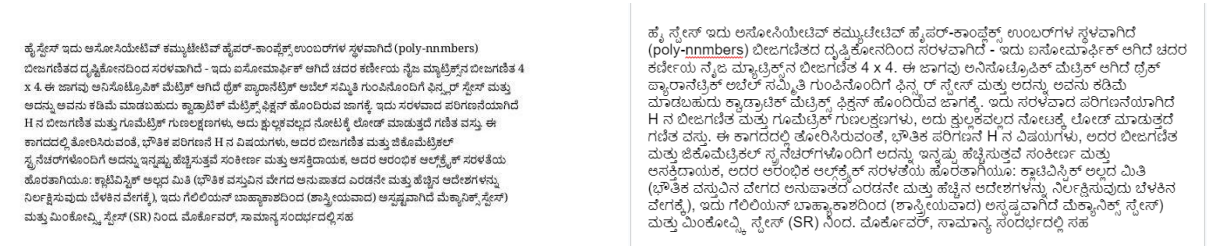

Figure 5: Kannada Document Processing: Comparison between the original document (left) and the model's OCR output (right)

A.3 Training Dynamics Analysis

A.3.1 Single Language LoRA Adaptation

We first analyze the training dynamics for individual languages using LoRA with rank=64 and α=128. Figure 6 shows the training curves for Hindi and Kannada.

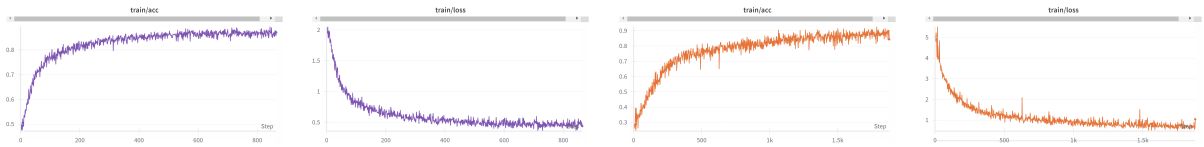

Figure 6: Single Language LoRA Training Dynamics: Training and loss curves for Hindi (purple) and Kannada (orange) using LoRA (r=64, α=128). Both languages show stable convergence patterns with Hindi achieving slightly faster convergence.

A.3.2 Multi-Language Joint Training

Building on the single language results, we investigate joint training on Hindi and Kannada. Figure 7 demonstrates the effectiveness of our multi-language approach.

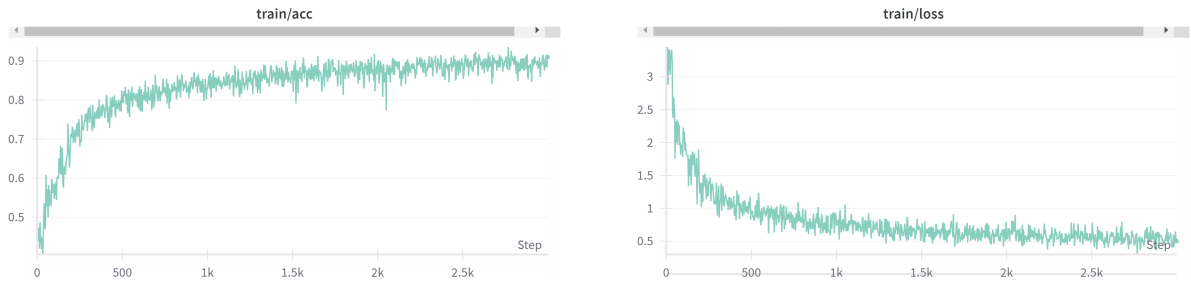

Figure 7: Joint Hindi-Kannada Training: The model maintains strong performance while learning both languages simultaneously, suggesting effective parameter sharing between related scripts.

A.3.3 Comparative Analysis of Joint vs Individual Training

To validate our multi-language approach, we compare joint training performance against individual language models. Figure 8 presents this critical comparison, where the orange line represents Kannada with rank 64 LoRA, the neon line shows the joint Hindi-Kannada LoRA (rank 64), and the green line indicates Hindi with rank 64 LoRA adaptation.

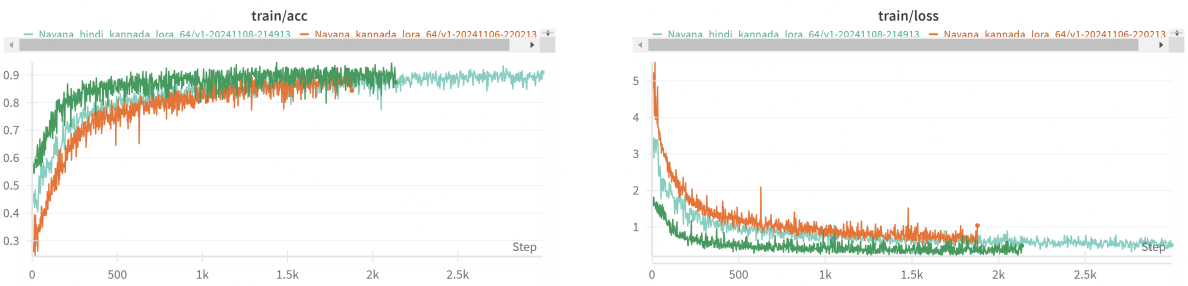

Figure 8: Comparative Analysis: Joint Hindi-Kannada training (r=64, α=128) versus individual language models. The joint model (neon) achieves comparable performance to individual Hindi (green) and Kannada (orange) models while using fewer parameters, demonstrating efficient cross-lingual transfer.

A.3.4 Vocabulary Expansion Experiments

Our initial experiments explored vocabulary expansion as a potential approach for handling multiple scripts. Figure 9 illustrates these challenges, comparing standard LoRA adaptation (purple lines) against vocabulary expansion attempts (grey lines).

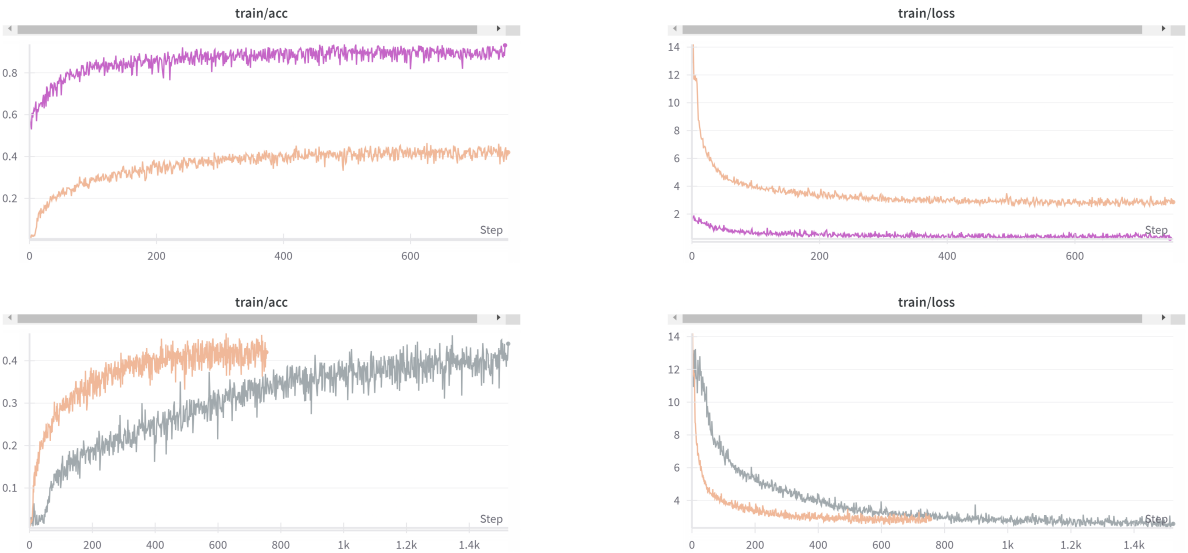

Figure 9: Vocabulary Expansion Analysis: Attempts to expand model vocabulary for Hindi showed poor convergence across different configurations. The standard vocabulary with LoRA adaptation (purple) proved more effective than expanded vocabulary approaches (grey), leading us to abandon the vocabulary expansion strategy.

A.4 Data Generation Examples

A.4.1 Page-Level Translation Examples

Our pipeline demonstrates robust translation capabilities while preserving document structure across all supported languages. Figures 10, 11, 12, 13 and 14 showcase these capabilities across different Indic scripts.

A.4.2 Section-Level Translation Examples

Figures 15, 16, 17 and 18 showcase section level translation capabilities across different Indic scripts.

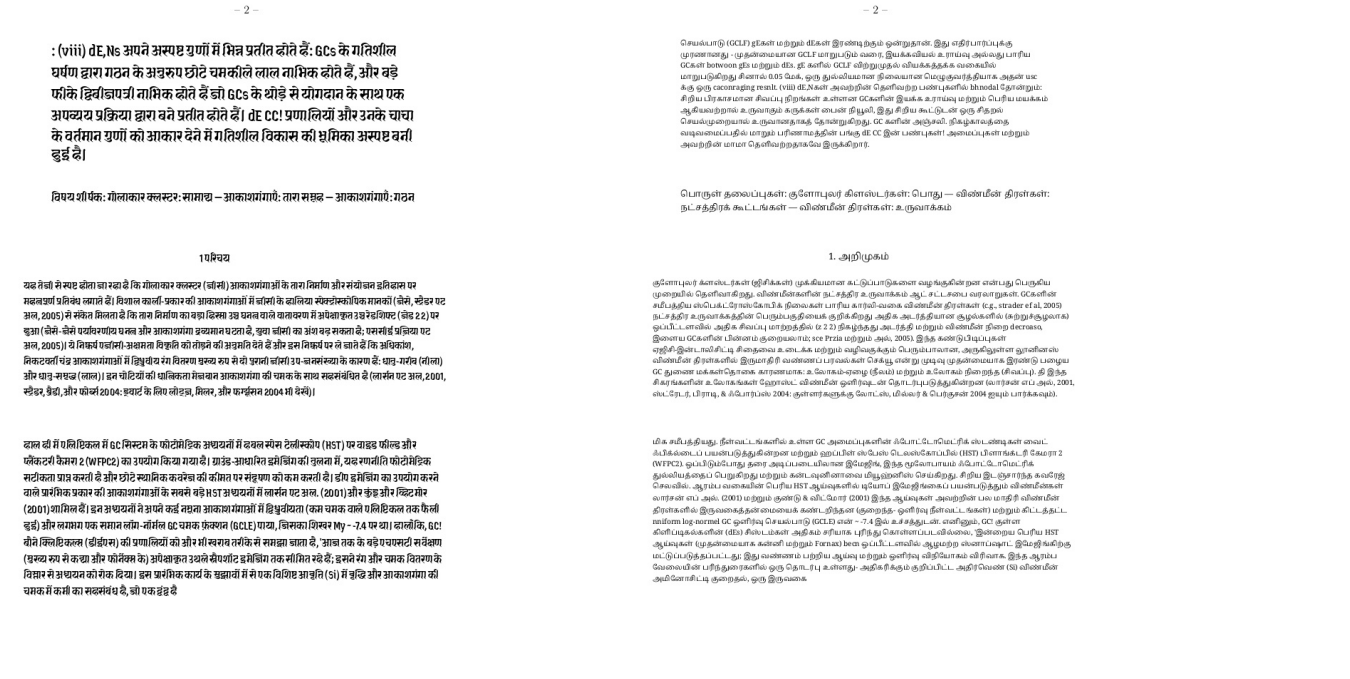

– 2 –

: (viii) dE,Ns अपने अस्पष्ट गुणों में भिन्न प्रतीत होते हैं: GCs के गतिशील घर्षण द्वारा गठन के अचरुप छोटे चमकीले लाल नाभिक होते हैं, और बड़े फीके द्विवीजपत्री नाभिक होते हैं ज्ञो GCs के थोड़े से योगदान के साथ एक अपव्यय प्रक्रिया द्वारा बने प्रतीत होते हैं। dE CC! प्रणालियों और उनके चाचा के वर्तमान गुणों को आकार देने में गतिशील विकास की भूमिका अस्पष्ट बनी हुई है।

विषय शीर्षक: गोलाकार क्लस्टर: सामान्य – आकाशगंगाएँ: तारा समूह – आकाशगंगाएँ: गठन

1 परिचय

यह तेज़ी से स्पष्ट होता जा रहा है कि गोलाकार क्लस्टर (जीसी) आकाशगंगा-प्रकों के तारा निर्माण और मंथन इतिहास पर महत्वपूर्ण प्रतिबंध लगाते हैं। विशाल काली-पदार्थ की आकाशगंगाओं में जीसी के द्वारिया स्पेक्ट्रोस्कोपिक मामलों (जैसे, स्टेडर एट अल, 2005) में संकेत मिलता है कि तारा निर्माण का बड़ा हिस्सा 3ख धनत्व वाले वातावरण में अपेक्षाकृत 3ख श्रेणिएट (जेड 2 2) पर ह्रआ (जैसे-जैसे पर्यावरणीय घनत्व और आकाशगंगा द्रव्यमान घटता है, युवा जीसी का अंश बढ़ सकता है; एमसीई प्रक्रिया एट अल, 2005)। ये निष्कर्ष एकसी-अक्षमता विकृति को तोड़ने की आवश्यकता देते हैं और इस निष्कर्ष पर ले जाते हैं कि अधिकांश, निकटवर्ती चंद्र आकाशगंगाओं में द्विघ्रवीय रुप विस्तृत घ्रस्य रुप से दो पुराने जीसी 3ख-जनसंख्या के कारण हैं: धातु-गरीब (नीला) और धातु-समृद्ध (लाल)। इन चोटियों की धालिकता मेजबान आकाशगंगा की चमक के साथ सहसंबंधित है (लार्सन एट अल,2001, स्टेडर, ईवी, और फोर्ब्स 2004: इसाएट के लिए लीइज़, मिलर, और फर्ग्यूसन 2004 भी देखें)।

दाल की में एलिप्टिकल में GC सिस्टम के फोटोमेट्रिक अध्ययनों में हबबल स्पेस टेलीस्कोप (HST) पर वाइड फील्ड और प्लैनेटरी कैमरा 2 (WFPC2) का उपयोग किया गया है। ग्राउंड-आधारित इमेजिंग की तुलना में, यह रणनीति फोटोमेट्रिक सटीकता प्राप्त करती है और छोटे स्थानिक कवरेज की कीमत पर संदूषण की कम करती है। हीण इमेजिंग का उपयोग करने वाले प्रारंभिक प्रकार की आकाशगंगाओं के सबसे बड़े HST अध्ययनों में लार्सन एट अल. (2001) और कुंड्रा और व्हिटमोर (2001) शामिल हैं। इन अध्ययनों ने अपने कई सदस्य आकाशगंगाओं में द्विघ्रवीयता (कम चमक वाले एलिप्टिकल तक फैली हुई) और लगभग एक समान लॉग-नॉर्मल GC चमक फ़ंक्शन (GCLE) पाया, जिसका शिखर My ~ -7.4 पर था। हालाँकि, GC! बीने क्लिप्टिकल्स (ईडीएस) की प्रणालियों को और भी स्वरान तरीके से समझा जाता है, 'आज तक के बड़े पयमारी मरक्षेण (सुस्थ रुप से कच्चा और फीनेक्स के) अपेक्षाकृत 3ख्ले सैपर्णाट इमेजिंग तक सीमित रहे हैं; इसने रंग और चमक वितरण के विज्ञान से अध्ययन को रोक दिया। इस प्रारंभिक कार्य के सुझावों में से एक विशिष्ट आ्रवृत्ति (Si) में वृद्धि और आकाशगंगा की चमक में कमी का सहसंबंध है, जो एक इंट्रड है

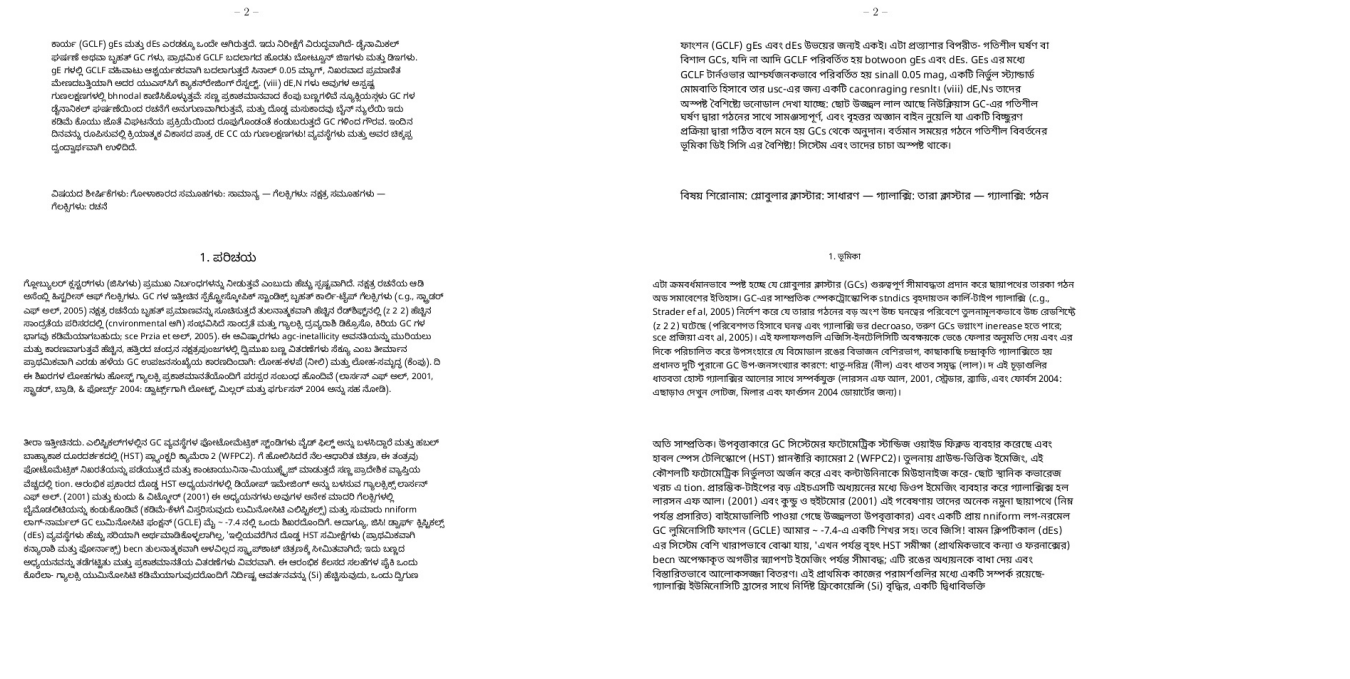

– 2 –

செயல்பாடு (GCLF) gEகள் மற்றும் dEகள் இரண்டிற்கும் ஒன்றுதான். இது எதிர்பாற்புக்கத் முரணானது - முதன்மையான GCLF மாறுபடும் வரை, இயக்கவியல் உராய்வு அல்லது பாரிய GCகள் botwoon gEs மற்றும் dEs. ஜீ களில் GCLF விற்றுமுதல் வியக்கத்தக்க வகையில் மாறுபடுகிறது சிஸாரல் 0.05 மேக், ஒரு துல்லியமான நிலையான மெழுகுவர்த்தியாக அதன் மங் கத் ஒரு ஒலமாதுழ rnslt. (viii) dE,Nகள் அவற்றின் தெளிவற்ற பண்புகளில் bhnodal தோன்றும்: சிறிய பிரகாசமான சிவப்பு நிறங்கள் உள்ளன GCகளின் இயக்க உராய்வு மற்றும் பெரிய மயக்கம் ஆகியவற்றால் உருவாகும் கருக்கள் பைன் நிழலி, இது சிறிய கூட்டுடன் ஒரு சீதநல் செயல்முறையால் உருவானதாகத் தோன்றுகிறது. GC களின் அஞ்சலி. நிகழ்காலத்தை வடிவமைப்பதில் மாறும் பரிணாமத்தின் பங்கு dE CC இன் பண்புகள்! அமைப்புகள் மற்றும் அவற்றின் மாமா தெளிவற்றதாகவே இருக்கிறார்.

பொருள் தலைப்புகள்: குளோபுலர் கிளஸ்டர்கள்: பொது — விண்மீன் திரள்கள்: நட்சத்திரக் கூட்டங்கள் — விண்மீன் திரள்கள்: உருவாக்கம்

1. அறிமுகம்

குளோபுலர் கிளஸ்டர்கள் (ஜிசிக்கள்) முக்கியமான கட்டுப்பாடுகளை வழங்குகின்றன என்பது பெருகிய முறையில் தெளிவாகிறது. விண்மீன்களின் நட்சத்திர உருவாக்கம் ஆட்சட்சபை வரவாறுகள். GCகளின் சமீபத்திய ஸ்பெக்ட்ரோஸ்கோபிக் நிலைகள் பாரிய கார்லி-வகை விண்மீன் திரள்கள் (e.g., strader el al, 2005) நட்சத்திர உருவாக்கத்தின் பெரும்பகுதியைக் குறிக்கிறது அதிக அடர்த்தியான சூழல்களில் (கற்றச்சூழலாக) ஒப்பிட்டளவில் அதிக சிவப்பு மாற்றத்தில் (z 2 2) நிகழ்கிறது அடர்த்தி மற்றும் விண்மீன் நிறை decroaso, இவைய GCகளின் பிரிவினம் குறைவடைகாம் ice Przia மற்றும் அல், 2005) இந்த கண்டுபிடிப்புகள் ஏறுநிச்-இடைநலிசிட்டி சிதைவை உடைக்க மற்றும் வழிவகுக்கும் பெருமபாயான, அருகிலுள்ள ஓர்னினஸ் விண்மீன் திரள்களில் இருமுனதிரி வண்ணப் பரவல்கள் செகபு என்று முடிவு முதன்மையாக இரண்டு பழைய GC துணை மக்கள்தொகை காரணமாக: உலோகம்-ஏழை (நீலம்) மற்றும் உலோகம் நிறைந்த (சிவப்பு). தி இந்த சிகரங்களின் உலோகங்கள் நோஸ்ட்ட் விண்மீன் ஒளிரவுடன் தொடர்புடுத்துகின்றன (லார்சன் எப் அல், 2001, ஸ்டேடர், பீராடி, & சிபாரம் 2004; குள்ளர்களுக்கு வோட்ட மில்லர் & பெருகான் 2004 ஐயும் பார்க்கவும்).

மிக சமீபத்தியது, நீள்வட்டங்களில் உள்ள GC அமைப்புகளின் ஸ்பேர்ட்டாமெட்ரிக் ஸ்பண்டிகள் வைட் ஃபீல்கமப் பயன்படுத்துகின்றன மற்றும் ஹப்பிளின் ஸ்பேஸ் டெலஸ்கோப்பில் (HST) பிளானெட்டரி கேமரா 2 (WFPC2) ஒப்பிடும்போது தனர ஆடியவியான இங்கிஜிங் இந்த சூலோபாயம் சிக்காட்டோமெட்ரிக் துல்லியத்தைப் பெறுகிறது மற்றும் கண்டவுனிளாலைவ மிஷுஎனிளிங் செய்கிறது. சிறிய இடஞ்சாராந்த கவரேஜு செலவில். ஆரம்ப வகையின் பெரிய HST ஆய்வுகளில் டியோப் இமேஜிங்கைப் பயன்படுத்தும் விண்மீண்கள் லார்சன் எப் அல். (2001) மற்றும் குண்டு & விட்மோர் (2001) இந்த ஆய்வுகள் அவற்றின் பல மாநிறி விண்மீன் திரள்களில் இருவகைத்தன்மையைக் கண்டறிந்தன (ஒளிநிரவு நீள்வட்டங்கள்) மற்றும் கிட்டத்தட்ட uniform log-normal GC ஒளிரவு செயல்பாடு (GCLD எனா ~ -7.4 இல் உச்சத்துடன். எனினும், GC துணை கிளிப்புக்கல்களின் (dEs) சிங்டம்கள் அதிகம் சரியாக யரிந்து கொள்ளப்படவில்லை. 'இன்னறைய பெரிய HST ஆய்வுகள் (முதன்மையாக கன்னி மற்றும் Fornax) bcn ஒப்பிட்டளவில் ஆழமற்ற எனாப்வதாட். இமேஜிங்கிற்கு மட்டுப்படுத்தப்பட்டது; இது வண்ணம் பற்றிய ஆய்வு மற்றும் ஒளிரவு விநியோகம் விரிவாக. இந்த ஆரம்ப வேலையின் பரிந்துரைகளில் ஒரு தொடர்பு உள்ளது- அதிகரிக்கும் குறிப்பிட்ட அதிரெவன (S) விண்மீன் அமினோசிட்டி குறைதல், ஒரு இடுவகை

Figure 10: Page-level translation examples showing Hindi (left) and Tamil (right) translations with preserved document layout.

– 2 –

ಕಾರ್ಯ (GCLF) gEs ಮತ್ತು dEs ಎರಡಕ್ಕೂ ಒಂದೇ ಆಗಿರುತ್ತದೆ. ಇದು ನಿರೀಕ್ಷೆಗೆ ವಿರುದ್ಧವಾಗಿದೆ- ಡೈನಾಮಿಕಲ್ ಘರ್ಷಣೆ ಅಥವಾ ಬೃಹತ್ GC ಗಳು, ಪ್ರಾಥಮಿಕ GCLF ಬದಲಾಗದೆ ಹೊರಬರುವ ಮೋಟಬ್ಬನ್ ಶಾಗಗಳು ಮತ್ತು ಡಿಗಾಗಳು. gE ಗಳಲ್ಲಿ GCLF ವಹಿವಾಟು ಆಶ್ಚರ್ಯಕರವಾಗಿ ಬದಲಾಗುತ್ತದೆ ಸಿನಾಲ್ 0.05 ಮ್ಯಾಗ್, ನಿಖರವಾದ ಪ್ರಮಾಣಿತ ಮೇಣದಬತ್ತಿಯಾಗಿ ಅದರ ಯುವಸ್ಸಿಗೆ ಕ್ಯೂಸನ್‌ರೇಂಜಿಂಗ್ ರೆಸ್ಟಲ್ಟ್. (viii) dE,N ಗಳು ಅವುಗಳ ಅಸ್ಪಷ್ಟ ಗುಣಲಕ್ಷಣಗಳಲ್ಲಿ bhnodal ಜಾತಿಸಿಕೊಳ್ಳುತ್ತವೆ: ಸಣ್ಣ ಪ್ರಕಾಶಮಾನವಾದ ಕೆಂಪು ಬಣ್ಣಗಳಿವೆ ನ್ಯೂಕ್ಲಿಯಸ್‌ಗಳು GC ಗಳ ಡೈನಾಮಿಕಲ್ ಘರ್ಷಣೆಯಿಂದ ರಚನೆಗೆಗೆ ಅನುಗುಣವಾಗಿರುತ್ತವೆ, ಮತ್ತು ದೊಡ್ಡ ಮಸುಕಾದವು ಬೈನ್ ನ್ಯೂಲೆಯ ಇದು ಕಠಿಮಿ ಕೊಯು ಜೊತೆ ವಿಘಟನೆಯ ಪ್ರಕ್ರಿಯೆಯಿಂದ ರೂಪುಗೊಂಡಂತೆ ಕಂಡುಬರುತ್ತದೆ GC ಗಳಿಂದ ಗಿರಿವೆ. ಇಂದಿನ ದಿನವನ್ನು ರೂಪಿಸುವಲ್ಲಿ ಕ್ರಿಯಾತ್ಮಕ ವಿಕಾಸದ ಮಾತ್ರ dE CC ಯ ಗುಣಲಕ್ಷಣಗಳು! ವೃದ್ಧರೈಗಳು ಮತ್ತು ಅವರ ಚಿಕ್ಕಪ್ಪ ದ್ವಂದ್ವಾರ್ಥವಾಗಿ ಉಳಿದಿದೆ.

ವಿಷಯದ ಶೀರ್ಷಿಕೆಗಳು: ಗೋಳಾಕಾರದ ಸಮೂಹಗಳು: ಸಾಮಾನ್ಯ — ಗೆಲಕ್ಸಿಗಳು: ನಕ್ಷತ್ರ ಸಮೂಹಗಳು — ಗೆಲಕ್ಸಿಗಳು: ರಚನೆ

1. ಪರಿಚಯ

ಗ್ಲೋಬ್ಯುಲರ್ ಕ್ಲಸ್ಟರ್‌ಗಳು (ಜಿಸಿಗಳು) ಪ್ರಮುಖ ನಿರ್ಬಂಧಗಳನ್ನು ನೀಡುತ್ತವೆ ಎಂಬುದು ಹೆಚ್ಚು ಸ್ಪಷ್ಟವಾಗಿದೆ. ನಕ್ಷತ್ರ ರಚನೆಯ ಆಡಿ ಅಸೆಂಬ್ಲಿ ಹಿಸ್ಟರೀಸ್ ಆಫ್ ಗೆಲಕ್ಸಿಗಳು. GC ಗಳ ಇತ್ತೀಚಿನ ಸ್ಪೆಕ್ಟ್ರೋಸ್ಕೋಪಿಕ್ ಸ್ಟ್ಯಾಡಿಜ್ ಬೃಹತ್ ಕಾರ್ಲೀ-ಟೈಪ್ ಗೆಲಕ್ಸಿಗಳು (e.g., ಸ್ಟ್ರಾಡರ್ ಎಫ್ ಅಲ್., 2005) ನಕ್ಷತ್ರ ರಚನೆಯ ಬೃಹತ್ ಪ್ರಮಾಣವನ್ನು ಸೂಚಿಸುತ್ತದೆ ತುಲನಾತ್ಮಕವಾಗಿ ಹೆಚ್ಚಿನ ರೆಡ್‌ಶಿಫ್ಟ್‌ನಲ್ಲಿ (z 2 2) ಹೆಚ್ಚಿನ ಸಾಂದ್ರತೆಯ ಪರಿಸರದಲ್ಲಿ (cnvironmental ಆಗಿ) ಸಂಭವಿಸಿದೆ ಸಾಂದ್ರತೆ ಮತ್ತು ಗ್ಯಾಲಕ್ಸಿ ದ್ರವ್ಯದಾಕಿ ತಿಳಿಸೊಂ, ತಿರಿಯ GC ಗಳ ಭಾಗವು ಕಠಿಮಿಯಾಗಬಹುದು; sce Przia et ಅಲ್, 2005). ಈ ಆವಿಷ್ಕಾರಗಳು agc-inetallicity ಅವನತಿಯನ್ನು ಮುರಿಯಲು ಮತ್ತು ಕಾರಣವಾಗುತ್ತವೆ ಹೆಚ್ಚಿನ, ಹತ್ತಿರದ ಚಂದ್ರನ ನಕ್ಷತ್ರಪುಂಜಗಳಲ್ಲಿ ದ್ವಿಮುಖ ಬಣ್ಣ ವಿತರಣೆಗಳು ನೆಕ್ಕೂ ಎಂಬ ತೀರ್ಮಾನ ಪ್ರಾಥಮಿಕವಾಗಿ ಎರಡು ಹಳೆಯ GC ಉಪಜನಸಂಖ್ಯೆಯ ಕಾರಣದಿಂದಾಗಿ: ಲೋಹ-ಕಳಪೆ (ನೀಲಿ) ಮತ್ತು ಲೋಹ-ಸಮೃದ್ಧ (ಕೆಂಪು). ದಿ ಈ ಶಿಖರಗಳ ಲೋಹಗಳು ಹೋಸ್ಟ್ ಗ್ಯಾಲಕ್ಸಿ ಪ್ರಕಾಶಮಾನತೆಯೊಂದಿಗೆ ಪರಸ್ಪರ ಸಂಬಂಧ ಹೊಂದಿವೆ (ಲಾರ್ಸನ್ ಎಫ್ ಅಲ್., 2001, ಸ್ಟ್ರಾಡರ್, ಬ್ಯಾಡಿ, & ಫೋರ್ಬ್ಸ್ 2004: ಡ್ವಾರ್ಫ್‌ಗಾಗಿ ಲೋಆಟ್ಸ್, ಮಿಲ್ಲರ್ ಮತ್ತು ಫರ್ಗುಸನ್ 2004 ಅನ್ನು ನೋಡಿ).

ತೀರಾ ಇತ್ತೀಚಿನದು. ಎಲಿಪ್ಟಿಕಲ್‌ಗಳಲ್ಲಿನ GC ವ್ಯವಸ್ಥೆಗಳ ಫೋಟೋಮೆಟ್ರಿಕ್ ಸ್ಟಂಡಿಗಳು ವೈಡ್ ಫೀಲ್ಡ್ ಅನ್ನು ಬಳಸಿದ್ದಾರೆ ಮತ್ತು ಹಬಲ್ ಬಾಹ್ಯಾಕಾಶ ದೂರದರ್ಶಕದಲ್ಲಿ (HST) ಪ್ಲಾನೆಟ್ರಿ ಕ್ಯಾಮೆರಾ 2 (WFPC2). ಗೆ ಹೋಲಿಸಿದರೆ ನೆಲ-ಆಧಾರಿತ ಚಿತ್ರಣ. ಈ ತಂತ್ರವು ಫೋಟೊಮೆಟ್ರಿಕ್ ನಿಖರತೆಯನ್ನು ಪಡೆಯುತ್ತದೆ ಮತ್ತು ಕಾಂಟಾಯುನಿಯಾ-ಮಿಯುಟ್ಸ್ ಮಾಡುತ್ತದೆ ಸಣ್ಣ ಪ್ರಾದೇಶಿಕ ವ್ಯಾಪ್ತಿಯ ವೆಚ್ಚದಲ್ಲಿ tion. ಆರಂಭಿಕ ಪ್ರಾಥರದ ದೊಡ್ಡ HST ಅಧ್ಯಯನಗಳಲ್ಲಿ ಡಿಯೆಂಆಗ್ ಇಮೇಜಿಂಗ್ ಅನ್ನು ಬಳಸುವ ಗ್ಯಾಲಕ್ಸಿಗಳ ಲಾರ್ಸನ್ ಎಫ್ ಅಲ್., (2001) ಮತ್ತು ಕುಂದು & ವಿಟ್ಮೋರ್ (2001) ಈ ಅಧ್ಯಯನಗಳು ಅವುಗಳ ಅನೇಕ ಮಾದರಿ ಗೆಲಕ್ಸಿಗಳಲ್ಲಿ ಬೈಮೊಡಲಿಟಿಯನ್ನು ಕಂಡುಕೊಂಡಿವೆ (ಕಠಿಮಿ-ಕೆಳಗೆ ವಿಸ್ತರಿಸುವುದು ಲುಮಿನೋಸಿಟಿ ಎಲಿಪ್ಟಿಕಲ್ಸ್) ಮತ್ತು ಸುಮಾರು nniform ಲಾಗ್-ನಾರ್ಮಲ್ GC ಲುಮಿನೋಸಿಟಿ ಫಂಕ್ಷನ್ (GCLE) ಮೈ ~ -7.4 ನಲ್ಲಿ ಒಂದು ಶಿಖರದೊಂದಿಗೆ. ಆದಾಗ್ಯೂ, ಜಿಸಿ! ಡ್ವಾರ್ಫ್ ಕ್ಲಿಪ್ಟಿಕಲ್ಸ್ (dEs) ವ್ಯವಸ್ಥೆಗಳು ಹೆಚ್ಚು ಸರಿಯಾಗಿ ಅರ್ಥಮಾಡಿಕೊಳ್ಳಲಾಗಿಲ್ಲ, 'ಇದ್ದಿಯವರೆಗಿನ ದೊಡ್ಡ HST ಸಮೀಕ್ಷೆಗಳು (ಪ್ರಾಥಮಿಕವಾಗಿ ಕನ್ಯಾರಾಶಿ ಮತ್ತು ಫೋರ್ನಾಕ್ಸ್) bcn ತುಲನಾತ್ಮಕವಾಗಿ ಆಳವಿಲ್ಲದ ಸ್ಕ್ಯಾಪರಾಟ್ ಚಿತ್ರಣಕ್ಕೆ ಸೀಮಿತವಾಗಿದೆ: ಇದು ಬಣ್ಣದ ಅಧ್ಯಯನವನ್ನು ತಡೆಗಟ್ಟುತು ಮತ್ತು ಪ್ರಕಾಶಮಾನತೆಯ ವಿತರಣೆಗಳ ವಿವರವಾಗಿ. ಈ ಆರಂಭಿಕ ಕೆಲಸದ ಸಲಹೆಗಳ ಪೈಕಿ ಒಂದು ಕೊರೆಲಾ- ಗ್ಯಾಲಕ್ಸಿ ಯುಮಿನೋಸಿಟಿ ಕಠಿಮಿಯಾಗುವುದರೊಂದಿಗೆ ನಿರ್ದಿಷ್ಟ ಆವರ್ತನವನ್ನು (Si) ಹೆಚ್ಚಿಸುವುದು, ಒಂದು ರ್ರಿಗುಣ

Figure 11: Page-level translation examples demonstrating Kannada (left) and Bengali (right) translations.

– 2 –

ഫംഗ്ഷൻ (GCLF) gE കൾക്കും dE കൾക്കും തുല്യമാണ്. ഇത് പ്രതിക്ഷിച്ചതിന് വിരുദ്ധമാണ്- ഡൈമെൻഷിയൽ GCLF വ്യത്യാസപ്പെടുന്നില്ലെങ്കിൽ, ചലനാത്മക ഘർഷണം അല്ലെങ്കിൽ വലിയ GC-കൾ ബൊട്ടുവൻ ജിള്ളകളും ഡിള്ളകളും. gE-കൾക്കിടയിൽ GCLF വിറ്റുവരവ് അതിശക്തിപ്പെടുന്ന രീതിയിൽ വ്യത്യാസപ്പെടുന്നു; സിറാത്ത് 0.05 മാഗ്, കൃത്യമായ യൂനിഫോർമ് ഡെക്ലൈനിയായി അതിന്റെ usc-യ്ക്ക് ഒരു caconraging resnlt. (viii) dE,N കൾ അവയുടെ അവൃക്തമായ ഗുണങ്ങളിൽ bhnodal കാണപ്പെടുന്നു; ചെറിയ കടും ചുവപ്പ് ഇനത്ത് ജിസിക്കളുടെ ചലനാത്മക ഘർഷണം മൂലമുള്ള രൂപീകരണവുമായി പൊരുത്തപ്പെടുന്ന അണുകേന്ദ്രങ്ങൾ, വലിയ മങ്ങൽ ബൈൻ നുലയേയ്, ചെറിയ കര-വിസർജ്ജന പ്രക്രിയയാൽ രൂപപ്പെടുത്തിയ കാണപ്പെടുന്നു ജിസികളിൽ നിന്നുള്ള ആദരവ്. ഇന്നത്തെ രൂപപ്പെടുത്തുന്നതിൽ ചലനാത്മക പരിണാമത്തിന്റെ പങ്ക് dE CC യുടെ പ്രോപ്പർട്ടികൾ! സിസ്റ്റങ്ങളും അവയുടെ അമ്മാവനും അവൃക്തമായി തുടരുന്നു.

വിഷയ തലക്കെട്ടുകൾ: ഗോളാകൃതിയിലുള്ള ക്ലസ്റ്ററുകൾ: പൊതുവായ — ഗാലക്സികൾ: നക്ഷത്രസമൂഹങ്ങൾ — ഗാലക്സികൾ: രൂപീകരണം

1. ആമുഖം

ഗ്ലോബുലാർ ക്ലസ്റ്ററുകൾ (ജിസികൾ) പ്രധാന നിയന്ത്രണങ്ങൾ വാഗ്ദാനം ചെയ്യുന്നതായി കൂടുതൽ വ്യക്തമാണ്. താരാപഥങ്ങളുടെ നക്ഷത്ര രൂപീകരണ ഓഡ് അസംബ്ലി ചരിത്രങ്ങൾ. GC-കളുടെ സമീപകാല സ്പെക്ട്രോസ്കോപ്പിക് സിറ്റേർഡിക്സ് നീരാകാമായ കാർബൺ-തരം ഗാലക്സികൾ (e.g., Strader ef al, 2005) നക്ഷത്ര രൂപീകരണത്തിന്റെ ആദിമഘട്ടം സൃഷ്ടിക്കുന്നു താരതമ്യേന ഉയർന്ന ചുവപ്പ് ഷിഫ്റ്റിൽ (z 2 2) ഉയർന്ന സാന്ദ്രതയുള്ള അന്തരീക്ഷത്തിൽ (പരിസ്ഥിതി പൊലെ) സാന്ദ്രവിച്ചു സാന്ദ്രതയും ഗാലക്സി മാസ് വിശേഷതയും, ഇളയ ജിസികളുടെ അംശം കുറഞ്ഞെക്കാം; sce Przia et അൽ, 2005). ഈ കണങ്ങത്തലുകൾ എങ്ങിനി-ഇനറ്റാലിസിറ്റി വീജനറസി തകർക്കാൻ അനുവദിക്കുകയും അതിലേക്ക് നയിക്കുകയും ചെയ്യുന്നു സമീപത്തെ ലൂമിനസ് ഗാലക്സികളിലെ ദ്വിമാധാൻ വർണ്ണ വിതരണങ്ങൾ സെക്കൂ അളന്ന് എന്നാണ് നിഗമനം. പ്രാഥമികമായി രണ്ട് പഴയ GC ഉപജനസംഖ്യകൾ മൂലമാണ്: ലോഹ-പാവം (നീല), ലോഹ-സമ്പന്നമായ (ചുവപ്പ്). വി ഈ കൊടുമുടികളുടെ ലോഹങ്ങൾ ആതിമമായ ഗാലക്സി ലൂമിനോസിറ്റിയുമായി ബന്ധപ്പെടുത്തിക്കൊണ്ടു (Larson ef al, 2001, Strader, ബ്രാഡി, & ഫോർബസ് 2004: ഡ്വാർഫുകൾക്ക് ലോറ്റ്സ്, മില്ലർ, കെർഗുസൺ 2004 എന്നിവയും കാണുക).

ഏറ്റവും പുതിയത്. നിർഘടുത്താകുന്നിയിലുള്ള ജിസി സിസ്റ്റങ്ങളുടെ ഫോട്ടോമെട്രിക് സ്വത്തുകൾ വൈഡ് ഫീൽഡ് ഉപയോഗിച്ചു ഹബിൾ ബഹിരാകാശ ദൂരദർശിനിയിൽ (HST) പ്ലാൻറി ക്യാമറ 2 (WFPC2). ഇതിനോട് താരതമ്യപ്പെടുത്തി ഗ്രൗണ്ട് അധിഷ്ഠിത ഇമേജിംഗ്, ഈ നൂതന ഫോട്ടോമെട്രിക് കൃത്യത നേടുകയും കോണ്ടൗണിനെയ മിനുസപ്പെടുത്തുകയും ചെയ്യുന്നു, ചെറിയ സ്പേഷ്യൽ കവറേജിന്റെ ചെലവിൽ. ആദ്യകാല തരത്തിലുള്ള വലിയ HST പഠനങ്ങളിൽ വിപി ഇമേജിംഗ് ഉപയോഗിക്കുന്ന ഗാലക്സികൾ ബർഗണ്ട് എപാണ്. (2001) കുണ്ടു & വിറ്റമോർ (2001) ഈ പഠനങ്ങൾ അവയുടെ പല സാമീപ്യ ഗാലക്സികളിലും ബൈമോഡാലിറ്റി കണ്ടെത്തി (താഴ്ന്ന വരെ നിമ്നോന്നത-ലൂമിനോസിറ്റി ക്ലസ്റ്റർ). ഈ എന്നാണ് നൈഫോം ലോഗ്-നോർമൽ ജിസി ലൂമിനോസിറ്റി ഫംഗ്ഷനും (ജിസി.എൻഎൽ) ഒരേ - -7.4 എന്ന കൊടുമുടിയോടെ. എന്നിരുന്നാലും, ജിസി! കുള്ളൻ ക്ലിപ്റ്റിക്കലുകളുടെ (dEs) സിസ്റ്റങ്ങൾ കൂടുതലാണ് മോശമായി മനസ്സിലാക്കിയിട്ടില്ല. 'ഇതുവരെയുള്ള വലിയ എച്ച്എസ്ടി സർവേകൾ (പ്രാഥമികമായി കന്യകയുടെയും ഫോർനാക്സിന്റെയും) bcn താരതമ്യേന ആഴം കുറഞ്ഞ സ്നാപ്പ്ഷോട്ട് ഇമേജിംഗിലേക്ക് പരിമിതപ്പെടുത്തിയിരിക്കുന്നു; ഇത് നിറത്തെ കുറിച്ചുള്ള പഠനത്തെ തടഞ്ഞു പ്രകാശ വിതരണങ്ങൾ വിശാലമായി, ഈ പ്രദേശ പ്രവർത്തനത്തിന്റെ നിർദ്ദേശങ്ങളിൽ ഒരു കോമാറ- ഗാലക്സി അമിനോസിറ്റി കൂടുതലുള്ളതിനോപ്പം നിർദ്ദിഷ്ട ആവൃത്തി (Si) വർദ്ധിക്കുന്നു, ഒരു ദ്വിതലം

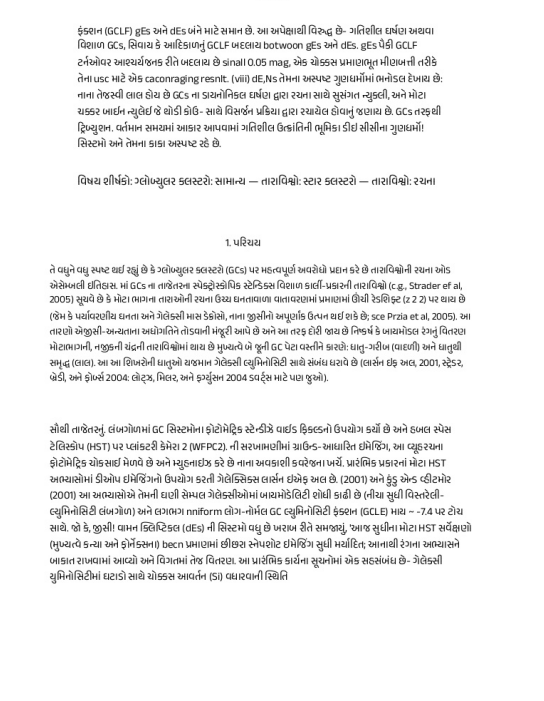

– 2 –

ફંક્શન (GCLF) gEs અને dEs બંને માટે સમાન છે. આ અપેક્ષાથી વિરુદ્ધ છે- ગતિશીલ ઘર્ષણ અથવા વિશાળ GCs, સિવાય કે આદિકાળનું GCLF બદલાય botwoon gEs અને dEs. gEs પેકી GCLF ટર્નઓવર આશ્ચર્યજનક રીતે બદલાય છે sinall 0.05 mag, એક યોક્કસ પ્રમાણમૂત મીણબત્તી તરીકે તેના usc માટે એક caconraging resnlt. (viii) dE,Ns તેમના અસ્પષ્ટ ગ્રુણધર્મોમાં ભનોડલ દેખાય છે: નાના તેજસ્વી લાલ હોય છે GCs ના ડાઝનોનિકલ ઘર્ષણ દ્વારા રચના સાથે સુસંગત ન્યુકલી, અને મોટા ચક્કર બાઈન ન્યુલેઈ જે થોડી કોઈ- સાથે વિસર્જન પ્રક્રિયા દ્વારા રચાયેલ હોવાનું જણાય છે. GCs તરફથી દ્વિધ્યુશન. વર્તમાન સમયમાં આકાર આપવામાં ગતિશીલ ઉત્ક્રાંતિની ભૂમિકા ડીઈ સીસીના ગ્રુણધર્મો! સિસ્ટમો અને તેમના કાકા અસ્પષ્ટ રહે છે.

વિષય શીર્ષક: ગ્લોબ્યુલર ક્લસ્ટરો: સામાન્ય — તારાવિશ્વો: સ્ટાર ક્લસ્ટરો — તારાવિશ્વો: રચના

1. પરિચય

તે વધુને વધુ સ્પષ્ટ થઈ રહ્યું છે કે ગ્લોબ્યુલર ક્લસ્ટરો (GCs) પર મહત્વપૂર્ણ અવશેષો પ્રદાન કરે છે તારાવિશ્વોની રચના ઓડ એસેમ્બલી ઇતિહાસ. માં GCs ના તાજેતરના સ્પેક્ટ્રોસ્કોપિક સ્ટેરિડક્સ વિશાળ કાર્લી-પ્રકારની તારાવિશ્વો (.g., Strader ef al, 2005) સૂચવે છે કે મોટા ભાગના તારાઓની રચના ઉચ્ચ ઘનતાવાળા વાતાવરણમાં પ્રમાણમાં લીથી રેડશિફ્ટ (z 2 2) પર થાય છે (જેમ કે પર્યાવરણિય ઘનતા અને ગેલેક્સી માસ ડેકોલો, તમારા જુસીની અપ્વાર્ઝ ઉત્પન્ન થઈ શકે છે; sce Przia et al, 2005). આ તારણો એજુસી-અચાનક અઘોગનિને તોડવાની મંજૂરી આપે છે અને આ તારુ દીઠી જાય છે નિષ્ઠર કે બાઝમોડલ રેગનું વિતરણ મોટામાગની, નજીકની યંદની તારાવિશ્વોમાં થાય છે મુખ્યત્વે બે જૂની GC પેઢા વસ્તીને કારણે: ધાતુ-ગરીબ (વાદળી) અને ધાતુથી સમૃદ્ધ (લાલ). આ આ રિશિગનેની ધાતુઓ ચશમાન ગેલેક્સી લ્યુમિનોસિટી સાથે સંબંધ ધરાયે છે (લાર્સન ઇફ અલ, 2001, સ્ટ્રેડર, બેડી, અને ફોબર્સ 2004: લોટ્ઝ, મિલર, અને કર્ગુસન 2004 કર્ટ્સ માટે પણ જુઓ).

સૌથી તાજેતર્મું. લંબગોળમાં GC સિસ્ટમોના ફોટોમેટ્રિક સ્ટેન્ડીઝે વાઈડ ફિલ્ડનો ઉપયોગ કર્યો છે અને ડબલ સ્પેસ ટેલિસ્કોપ (HST) પર પ્લાંકટરી કેમેરા 2 (WFPC2). ની સરખામણીમાં ગ્રાઉન્ડ-આધારિત ઈમેજિંગ, આ વ્યૂહરચના ફોટોમેટ્રિક યોકસાઈ મેળવે છે અને મ્યુકનાઇઝ કરે છે નાના અવકાશી કવરેજના ખર્ચે. પ્રારંભિક પ્રકારનાં મોટા HST અભ્યાસોમાં ડીબીપ ઇમેજિંગનો ઉપયોગ કરતી ગેલેક્સિક્સ લાર્સન ઇએફ અલ છે. (2001) અને કુંડુ એન્ડ વીટમોર (2001) આ અભ્યાસોએ તેમની દ્વારી સેમ્પલ ગેલેક્સીઓમાં બાયમોડેલિટી શોધી કાઢી છે (નીચા સુધી વિસ્તરેલી-લ્યુમિનોસિટી લંબગોળ) અને લગભગ nniform લોગ-નોર્મલ GC લ્યુમિનોસિટી ફંક્શન (GCLE) માય - -7.4 પર ટોચ સાથે. જો કે, જીસી! વામન ક્લિપ્ટિકલ (dEs) ની સિસ્ટમો વધુ છે ખરાબ રીતે સમજાયું, 'આજ સુધીના મોટા HST સર્વેક્ષણો ભુખ્યત્વે 5-ચા અને ફોર્નેક્સના becn પ્રમાણમાં લીંછવા સ્નેપશોટ ઇમેજિંગ સુધી મર્યાદિત; આનાથી રંગના આવાસને બાકાત રાખવામાં આવ્યો અને વિગતમાં તંજ વિતરણ. આ પ્રારંભિક કાર્યના સુસંબંધ છે- ગેલેક્સી યુમિનોસિટીમાં ઘટાડો સાથે યોક્કસ આવર્તન (Si) વધારવાની સ્થિતિ

Figure 12: Page-level translation examples showing Malayalam (left) and Gujarati (right) translations.

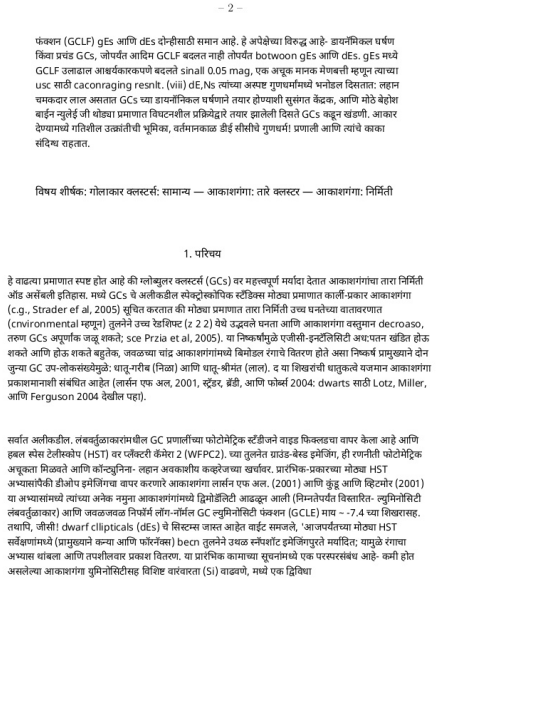

– 2 –

फंक्शन (GCLF) gEs आणि dEs दोन्हीसाठी समान आहे. हे अपेक्षेच्या विरुद्ध आहे- डायनॅमिकल घर्षण किंवा प्रचंड GCs, जोपर्यंत आदिम GCLF बदलत नाही तोपर्यंत bootwoon gEs आणि dEs. gEs मध्ये GCLF उलाढाल आश्चर्यकारकपणे बदलते sinall 0.05 mag, एक अचूक मानक मेणबत्ती म्हणून त्याच्या usc साठी caconraging resnlt. (viii) dE,Ns त्यांच्या अस्पष्ट गुणधर्मामध्ये भनोडल दिसतात: लहान चमकदार लाल असतात GCs च्या डायनॉमिकल घर्षणाने तयार झाल्याची सुसंगत केंद्रक, आणि मोठे बेहोश बाईन न्युलेई जी थोड्या प्रमाणात विघटनशील प्रक्रियेद्वारे तयार झालेली दिसते GCs कडून खंडणी. आकार देण्यामध्ये गतिशील उत्क्रांतीची भूमिका, वर्तमानकाळ डीई सीसीचे गुणधर्म! प्रणाली आणि त्यांचे काका संदिग्ध राहतात.

विषय शीर्षक: गोलाकार क्लस्टर्स: सामान्य — आकाशगंगा: तारे क्लस्टर — आकाशगंगा: निर्मिती

1. परिचय

हे वाढत्या प्रमाणात स्पष्ट होत आहे की ग्लोब्युलर क्लस्टर्स (GCs) वर महत्त्वपूर्ण मर्यादा देतात आकाशगंगांचा तारा निर्मिती ऑड असेंबली इतिहास, मध्ये GCs चे अलीकडील स्पेक्ट्रोस्कोपिक स्टेडिक्स मोठ्या प्रमाणात कार्ली-प्रकार आकाशगंगा (c.g., Strader ef al, 2005) सूचित करतात की मोठ्या प्रमाणात तारा निर्मिती उच्च घनतेच्या वातावरणात (cnvironmental म्हणून) तुलनेने उच्च रेडशिफ्ट (z 2 2) येथे उद्भवले घनता आणि आकाशगंगा वस्तुमान decroaso, तरुण GCs अपूर्णांक जळू शकते; sce Przia et al, 2005). या निष्कर्षांमुळे एजीसी-इन्टेलिजेंट अधःपतन खंडित होऊ शकते आणि होऊ शकते बहुतेक, जवळच्या चांद्र आकाशगंगांमध्ये द्विमोडेलिटी आढळून आली (निम्नतेपर्यंत विस्तारित- ल्युमिनोसिटी लंबवर्तुळाकार) आणि जवळजवळ निफॉर्म लॉग-नॉर्मल GC ल्युमिनोसिटी फंक्शन (GCLE) माय - -7.4 च्या शिखरासह. तथापि, जीसी! dwarf cllipticals (dEs) चे सिस्टम्स जास्त आहेत वाईट समजले, 'आजपर्यंतच्या मोठ्या HST सर्वेक्षणांमध्ये (प्राथमिक्या कन्या आणि फॉर्नॅक्स) becn तुलनेने उथळ स्नॅपशॉट इमेजिंगपुरते मर्यादित; यामुळे रंगाचा अभ्यास थांबला आणि तपशीलवार प्रकाश वितरण. या प्रारंभिक कामाच्या सूचनांमध्ये एक परस्परसंबंध आहे- कमी होत असलेल्या आकाशगंगा युमिनोसिटीसह विशिष्ट वारंवारता (Si) वाढवणे, मध्ये एक द्विधिया

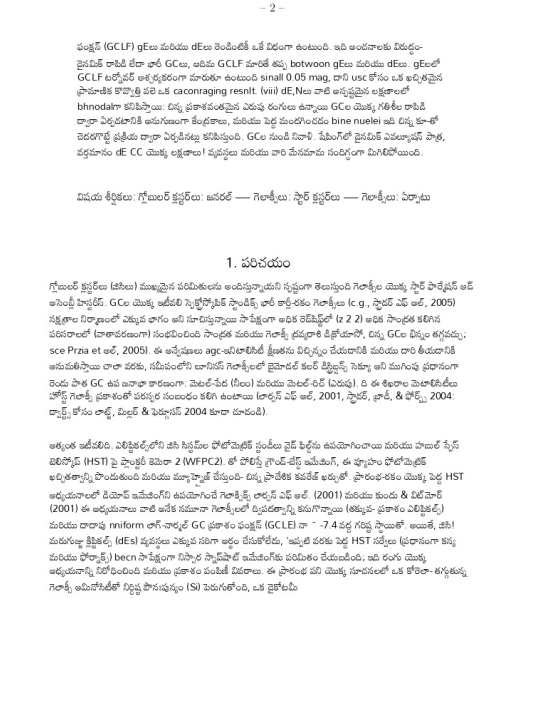

– 2 –

పంక్షన్ (GCLF) gEలు మరియు dEలు రెండింటికీ ఒకే విధంగా ఉంటుంది. ఇది ఆంచనాలకు విరుద్ధం- డైనమిక్ రాపిడి లేదా భారీ GCలు, అదిమ GCLF మారితే తప్ప botwoon gEలు మరియు dEలు. gEలలో GCLF టర్నోవర్ ఆశ్చర్యకరంగా మారుతూ ఉంటుంది sinall 0.05 mag, దాని usc కోసం ఒక ఖచ్చితమైన ప్రామాణిక కొవ్వొత్తి పని ఒక caconraging resnlt. (viii) dE,Nలు వాటి అస్పష్టమైన లక్షణాలలో bhnodalగా కనిపిస్తాయి: దున్న ప్రకాశవంతమైన ఎరుపు రంగులు ఉన్నాయి GCల యొక్క గతిశీల రాపిడి ద్వారా ఏర్పడటానికి అనుగుణంగా కేంద్రకాలు, మరియు పెద్ద మందగించడం bine nuelei ఇది లిన్న కూతో చెదరగొట్టే ప్రక్రియ ద్వారా ఏర్పడినట్లు కనిపిస్తుంది. GCల నుండి నివాళి. మేపింగ్ లో డైనమిక్ ఎవల్యూషన్ పాత్ర, వర్తమానం dE CC యొక్క లక్షణాలు! మృదువైన మరియు వారి మేనమామ సందిగ్ధంగా మిగిలిపోయింది.

విషయ శీర్షికలు: గ్లోబులర్ క్లస్టర్‌లు: జనరల్ — గెలాక్సీలు: స్టార్ క్లస్టర్‌లు — గెలాక్సీలు: ఏర్పాటు

1. పరిచయం

గ్లోబులర్ క్లస్టర్‌లు (జిసిలు) ముఖ్యమైన పరిమితులను అందిస్తున్నాయని స్పష్టంగా తెలుస్తుంది గెలాక్సీల యొక్క స్టార్ ఫార్మేషన్ ఆడ్ అసెంబ్లీ హిస్టరీ. GCల యొక్క ఇటీవలి స్పెక్ట్రోస్కోపిక్ స్టాండిక్స్ భారీ కార్లీ-రకం గెలాక్సీలు (e.g., స్ట్రాడర్ ఎఫ్ అల్, 2005) నక్షత్రాల నిర్మాణంలో ఎక్కువ భాగం జని సూచిస్తున్నాయి సాపేక్షంగా అధిక రెడ్‌షిఫ్ట్‌లో (z 2 2) అధిక సాంద్రత కలిగిన పరిసరాలలో (వాతావరణంగా) సంభవించింది సాంద్రత మరియు గెలాక్సీ ద్రవ్యరాశి డీజోయాస్తో, దున్న GCల చిన్నం తగ్గవచ్చు; sce Przia et అల్, 2005). ఈ అన్వేషణలు agc-జనిలలిటీ క్షీణతను విచ్ఛిన్నం చేయడానికి మరియు దారి తీయడానికి అనుమతిస్తాయి చాలా వరకు, సమీపంలోని బాగినస్ గెలాక్సీలలో డైమోడల్ కలర్ డిస్ట్రిబ్యూన్ సెమ్మూ జని ముగింపు ప్రధానంగా రెండు పాత GC ఉప జనాభా కారణంగా: మెటల్-పేద (నీలం) మరియు మెటల్-రిచ్ (ఎరుపు). ది ఈ శిఖరాల మెటాలిసిటీలు హోస్ట్ గెలాక్సీ ప్రకాశంలో పరస్పర సంబంధం కలిగి ఉంటాయి (లార్సన్ ఎఫ్ అల్, 2001, స్ట్రాడర్, బ్రాడీ, & ఫోర్బ్స్ 2004: డ్వార్ఫ్స్ కోసం లాట్జ్, మిల్లర్ & ఫెర్గుసన్ 2004 కూడా చూడండి).

ఆత్యంత ఇటీవలిది. విశిష్టికల్స్‌లోని జసి సిస్టమ్‌ల ఫోటోమెట్రిక్ స్టంట్‌లు వైడ్ ఫీల్డ్‌ను ఉపయోగించాయి మరియు హబుల్ స్పేస్ టెలిస్కోప్ (HST) పై ప్లాంక్టర్ కెమెరా 2 (WFPC2). భూ పోలిస్తే గ్రౌండ్-బేస్డ్ ఇమేజింగ్, ఈ వ్యూహం ఫోటోమెట్రిక్ ఖచ్చితత్వాన్ని పొందుతుంది మరియు మ్యూన్హ్యాక్ చేస్తుంది- దున్న ప్రాదేశిక కవరేజ్ ఖర్చుతో. ప్రారంభ-రకం యొక్క పెద్ద HST ఆధ్యయనాలలో డీయాప్ ఇమేజింగ్‌ని ఉపయోగించే గెలాక్సీల్స్ లార్సన్ ఎఫ్ అల్. (2001) మరియు కుండు & విట్‌మార్ (2001) ఈ ఆధ్యయనాన్ని బాటి ఇనేక నమూనా గెలాక్సీలలో బైమోడల్‌ను కనుగొన్నాయి (తక్కువ- ప్రకాశం ఎలిప్టికల్స్) మరియు దాదాపు nniform లాగ్-నార్మల్ GC ప్రకాశం ఫంక్షన్ (GCLE) నా - -7.4 వద్ద గరిష్ట స్థాయితో. అయితే, జసి! మరుగుజ్జు క్లిప్టికల్స్ (dEs) వ్యవస్థలు ఎక్కువ సరిగా అర్థం చేసుకోలేదు, 'ఇప్పటి వరకు పెద్ద HST సర్వేలు (ప్రధానంగా కన్య మరియు ఫోర్నాక్స్) bcn స్నాప్‌షాట్ ఇమేజింగ్‌కు పరిమితం చేయబడింది, ఇది రంగు యొక్క ఆధ్యయనాన్ని నిరోధించింది మరియు ప్రకాశం పంపిణీ విస్తరాలు. ఈ ప్రారంభ పని యొక్క సూచనలలో ఒక కోరికా- తగ్గుతున్న గెలాక్సీ ఆమినోసిటీతో నిర్దిష్ట పౌనఃపున్యం (Si) పెరుగుతోంది, ఒక డైకోటమీ

Figure 13: Page-level translation examples demonstrating Marathi (left) and Telugu (right) translations.

Figure 14: Page-level translation examples showing Odia (left) and Punjabi (right) translations.

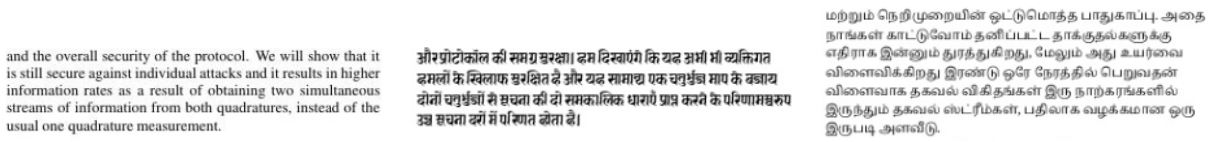

Figure 15: Section-level translation examples showing English (original), Hindi, and Tamil translations.

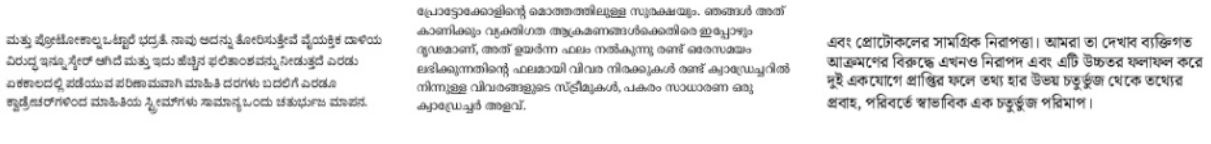

Figure 16: Section-level translation examples showing Kannada, Malayalam, and Bengali translations.

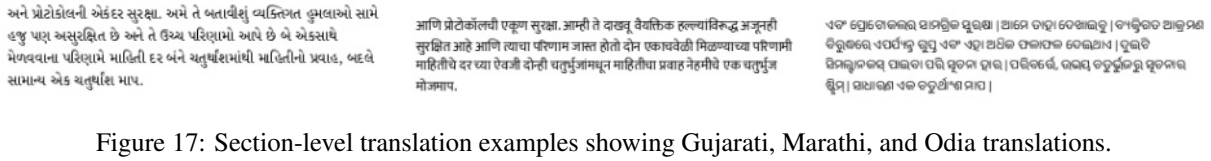

Figure 17: Section-level translation examples showing Gujarati, Marathi, and Odia translations.

Figure 18: Section-level translation examples showing Punjabi and Telugu translations.

A.5 Data Augmentation Examples

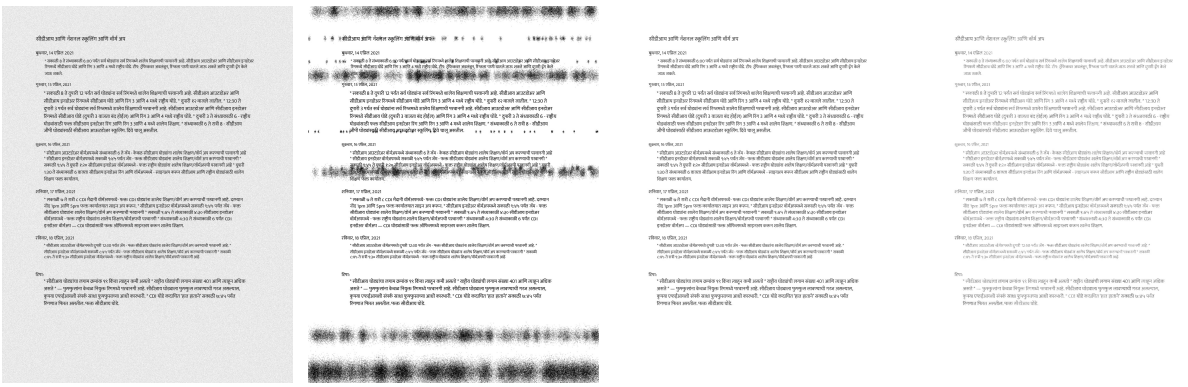

Figure 19: Document degradation examples showing (from left to right): background texturization, printer drum defects, ink mottling effect, and letterpress impression.

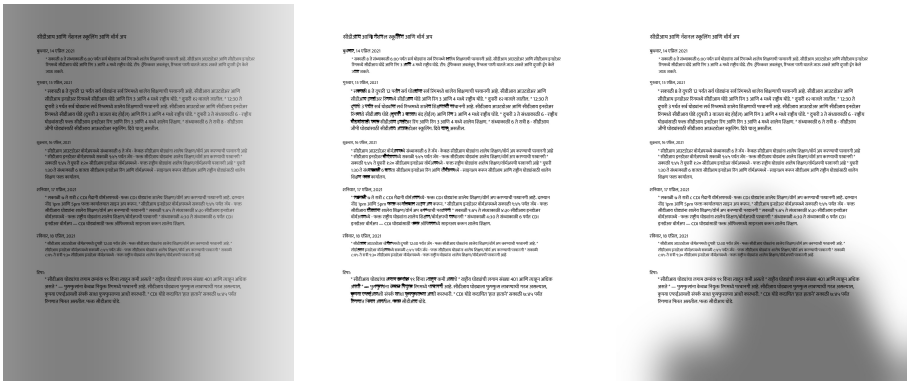

Figure 20: Document degradation examples showing (from left to right): lighting gradient, line degradation, shadow effects, and ink bleeding.